

Species of the genus *Gomphonema* from Haqlan hot springs, Iraq, with the description of two new species

ADIL Y. AL-HANDAL ^{1*}, ZLATKO LEVKOV ², HUDA ABDULLAH³ & ANGELA WULFF ¹

¹Department of Biological and Environmental Sciences, Faculty of Science, University of Gothenburg, Gothenburg, Sweden

²Institute of Biology, Faculty of Natural Sciences, Ss. Cyril and Methodius University, Skopje, Macedonia

³Department of Hadithah Education, General Directorate of Education in Anbar, Ministry of Education, Anbar, Iraq

This work presents a systematic account of the species of *Gomphonema* in Haqlan hot springs, Iraq. In diatom-rich material epiphytic on the aquatic plant *Najas minor*, 11 species belonging to *Gomphonema* were encountered, including two species new to science: *G. brockiae* sp. nov. and *G. hadithaensis* sp. nov. These species were described based on light and electron microscope observations. *Gomphonema brockiae* is a thermophilic and halophilic species, differentiated from its allied taxa by valve morphology and ultrastructure, including valve outline and size, stria density and areola shape. *Gomphonema hadithaensis* is characterized by its naviculoid shape and large size but can be distinguished from related taxa by its length/width ratio as well as stria density. A detailed morphological description of valve ultrastructure is provided for all species in this work. Eight of the currently identified *Gomphonema* species are new records for Iraq. This work is a documentation of diatoms present in a rapidly changing habitat due to severe shortage of freshwater supply to Iraq.

Keywords: diatoms, epiphytic, freshwater, new species, taxonomy

Introduction

Gomphonema Ehrenberg is a largely diversified biraphid diatom genus characterized by having linear-lanceolate to elliptical heteropolar to almost isopolar valves. The valves are apically asymmetric with the head pole usually wider than the basal pole (Round et al. 1990). According to Kociolek et al. (2019), *Gomphonema* encompasses 2400 taxa distributed worldwide in a variety of freshwater environments including oligotrophic, eutrophic and organically polluted water bodies. This large species number includes many taxa that have not been critically examined and verified. Guiry & Guiry (2024) estimated that 461 species of *Gomphonema* are of uncertain identities.

Species of *Gomphonema* are common in benthic diatom communities and many are of cosmopolitan distribution with varying life forms such as epiphytic, epipelagic, epipsammic and epilithic (Reichardt 2001, 2008, 2015, Levkov et al. 2016). Such a diversified nature of the genus representatives with wide morphological and structural variations creates taxonomic problems (Krammer & Lange-Bertalot 1991). Morphological variations include raphe structure (straight or lateral), curvature of the raphe endings, presence or absence of isolated pores (stigmata), mono- or biseriata striae, occluded or un-occluded areolae,

presence and position of pseudosepta, besides other ultrastructural differences. To overcome part of this problem, molecular investigations on some of the highly variable species complexes were implemented and revealed numerous conspecific and wrongly identified species (Abarca et al. 2014, 2020, Jahn et al. 2017). Based on scanning electron microscope (SEM) observations and molecular analyses, certain *Gomphonema* species were transferred to other known genera such as *Gomphoneis* Cleve, and *Gomphonella* Rabenhorst (Jahn et al. 2017), or to newly-erected genera such as *Pseudogomphonema* Medlin, *Gomphonemopsis* Medlin, *Gomphoseptatum* Medlin (Medlin & Round 1986), *Gomphosinica* Kociolek, Q.-M.You, Q.-X.Wang & Q.Liu (2015) and *Indiconema* Karthick & Kociolek (in Karthick et al. 2023).

In mid- and north Iraq, a large network of freshwater systems covers the region, consisting of the two major rivers of Mesopotamia, Tigris and Euphrates, with tens of their tributaries and branches. Despite such an extensive river network and wetlands, information on diatom diversity and distribution are rare. The study of diatoms in the region was initiated by Kolbe & Kreiger (1942) who examined algal material collected during the Handels-Mazetti Expedition in 1910 from the Kurdistan area and reported

*Corresponding author. E-mail: adil.yousif@bioenv.gu.se

Associate Editor: Aleksandra Maria Zgrundo

(Received 4 July 2024; accepted 31 October 2024)

© 2024 The Author(s). Published by Informa UK Limited, trading as Taylor & Francis Group.

This is an Open Access article distributed under the terms of the Creative Commons Attribution License (<http://creativecommons.org/licenses/by/4.0/>), which permits unrestricted use, distribution, and reproduction in any medium, provided the original work is properly cited. The terms on which this article has been published allow the posting of the Accepted Manuscript in a repository by the author(s) or with their consent.

only four *Gomphonema* taxa. Three decades later, Hirano (1973) investigated the diatoms in samples collected from small rivers and springs obtained by the Botanical Expedition in 1970. He added two more *Gomphonema* species to the list of Kolbe & Kreiger (1942). *Gomphonema* taxa reported by these authors were *G. acuminatum* Ehrenberg, *G. angustatum* (Kützing) Rabenhorst, *G. constrictum* Ehrenberg, *G. intricatum* Kützing, *G. lanceolatum* C. Agardh, *G. olivaceum* (Hornemann) Brébisson and *G. parvulum* (Kützing) Kützing. More recent investigations on diatoms made by Hinton & Maulood (1979a, b) and Maulood & Hinton (1979) did not add any further *Gomphonema* taxa to the previous list. An additional number of *Gomphonema* species appeared in several recent graduate dissertations on the algae of mid- and north Iraq, but these were not accompanied by proper descriptions or clear images which make their identification questionable.

The present study is a taxonomic documentation of the epiphytic *Gomphonema* species found in a hot spring in the northern half of Iraq. We report 11 species of *Gomphonema*, most of which were not previously reported from Iraq, including the description of two species new to science, *G. brockiae* sp. nov. and *G. hadithaensis* sp. nov. A detailed description with light microscope (LM) and scanning electron microscope images are provided for all species. The description of the well documented and cosmopolitan *Gomphonema* species found in the present material is provided here to illustrate minor morphological variations between populations in different geographic locations. The material examined was rich in diatom taxa exhibiting other new and interesting species of other genera which will be dealt with separately.

Material and methods

Study site

Haqlan springs (34° 05' 27'' N, 42° 21' 57'' E) are small water impoundments located on the west side of Euphrates River at Haditha Town, 250 km north-west of Baghdad (Fig. 1). The springs receive underground water which passes through gypsum rocks giving them their natural high sulphate content. Water from the springs flow at 25 m³/sec, discharging into the Euphrates River proper and altering the water quality in that region (Zydan *et al.* 2007). The springs are located in the vast Haqlan dry valley, which occupies an area of 441 km² and has an elevation of 325 m above sea level. The water level is rather shallow, not exceeding 3 m in depth, and the bottom is composed of silt to sand. The edge of the springs is covered with patches of filamentous cyanobacteria and macrophytes.

Environmental factors

Determination of some physical and chemical factors in the study site were either measured *in situ* or in the laboratory

following APHA (2017). These include water temperature, pH, conductivity, turbidity, alkalinity, and concentrations of chloride, nitrate, phosphate and sulphate.

Samples and preparation

Samples were collected in January–March 2018 by cutting parts of the submerged aquatic plants in the shallow parts of the spring. The dominant aquatic plant was *Najas minor* which inhabits the shallow parts of the hot springs. The plants were collected by hand, placed in small plastic bottles and preserved with 4% formalin. Diatoms were cleaned by boiling the samples in 35% hydrogen peroxide for 15 minutes. A few drops of 50% hydrochloric acid were added to remove carbonate. After several rinses with deionized water, diatom samples were air dried on coverslips and then mounted in Naphrax. Light microscope examination and morphometric measurements were performed with a Zeiss Axioplan 2 microscope (Carl Zeiss AB) using differential interference contrast objectives (DIC). For SEM observations, a few drops of the cleaned diatom suspension were left to dry on an aluminium stub and examined in a Zeiss Ultra 55 FEG SEM (Chalmers University, Gothenburg, Sweden). The terminology used in the valve morphological and structural descriptions follows Ross *et al.* (1979), Round *et al.* (1990) and Levkov *et al.* (2016). The term 'Frequent' used in this study indicates more than 50 cells observed on each slide examined, 'Rare' refers to less than ten cells.

Results

Average water temperature during sampling period (January–March) was 31°C, pH values remained on the alkaline side and averaged 7.85. Electric conductivity was 4222 µS/cm, turbidity (NTU) 0.6, alkalinity (CaCO₃) 140 mg/L, chloride 336 mg/L, phosphate 0.16 µg at P-PO₄/l and sulphate 2040 mg/L.

Gomphonema acuminatum Ehrenberg (Figs 2–7, 78–87)

Krammer & Lange-Bertalot (1986), p. 365, pl. 160, figs 1–12, Levkov *et al.* (2016), p. 22, pl. 1, figs 1–14, pl. 2, figs 1–7, pl. 3, figs 1–14, pl. 4, figs 1–6.

Morphology. Valves strongly heteropolar, clavate, gibbous in centre with two constrictions. Head pole wedge-shaped, widens below apex and terminates in apiculate end. Base pole narrowly rounded. Valves 41–58 µm long, 10–11 µm wide at mid-valve. Axial area narrow, linear. Central area small, irregularly shaped, surrounded by alternating short and long striae. Isolated pore small, round, located at end of a long central stria. Raphe lateral, undulated, proximal raphe endings expanded, slightly deflected towards isolated pore. Striae radiate all over, becoming convergent near the poles, 11–13 in 10 µm at mid valve, 14–15 in 10 µm towards poles. In the SEM, externally, proximal

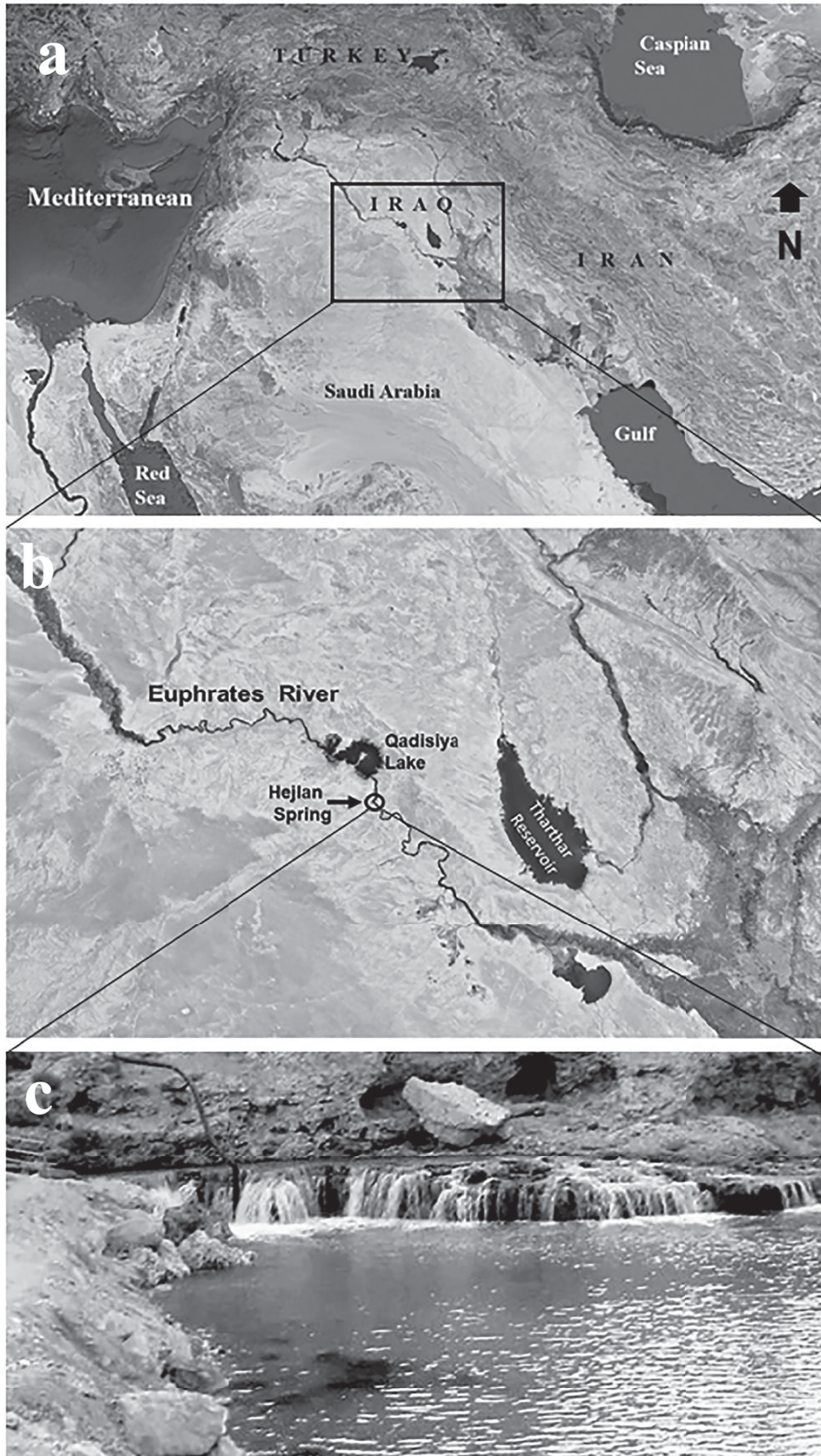
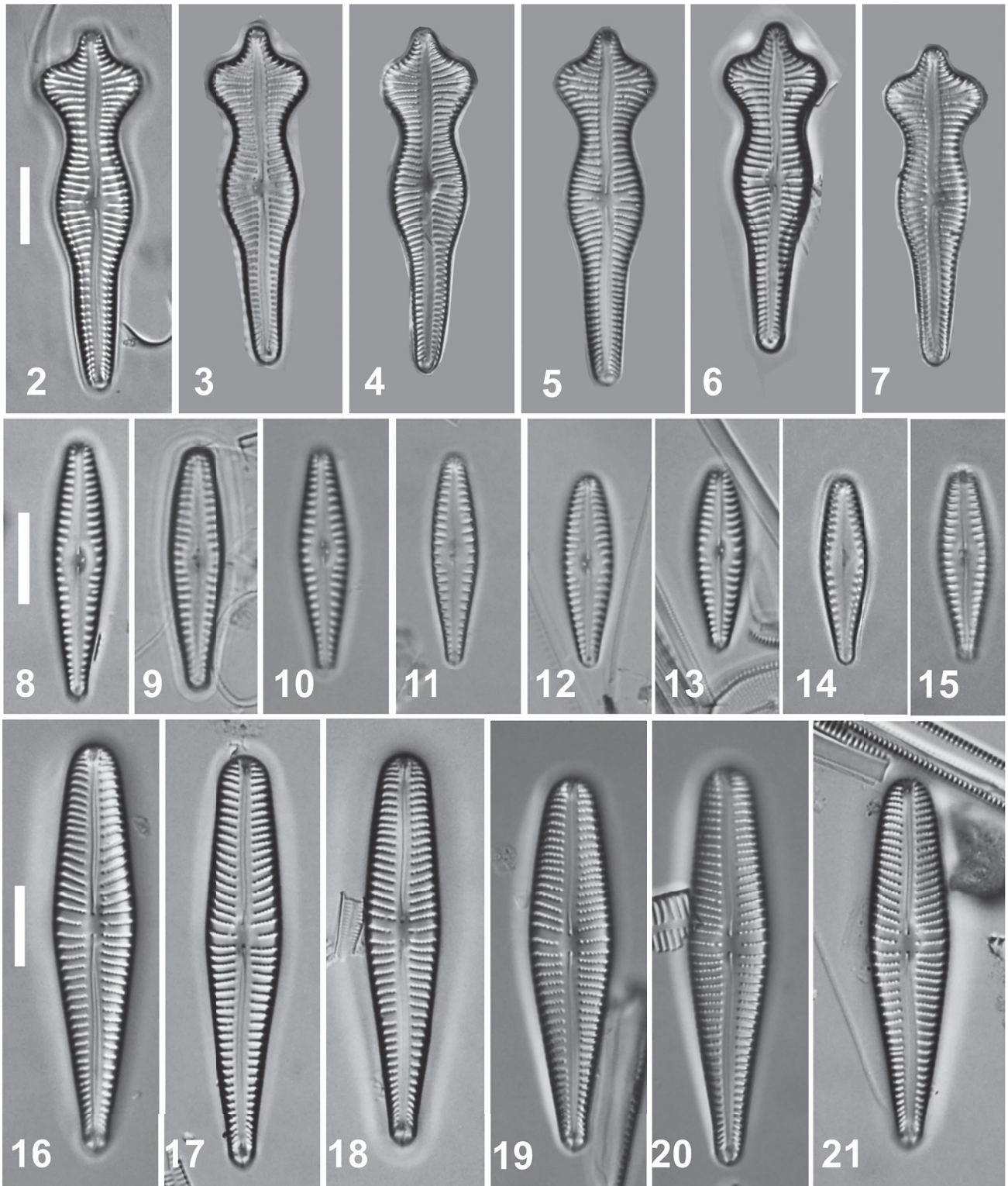
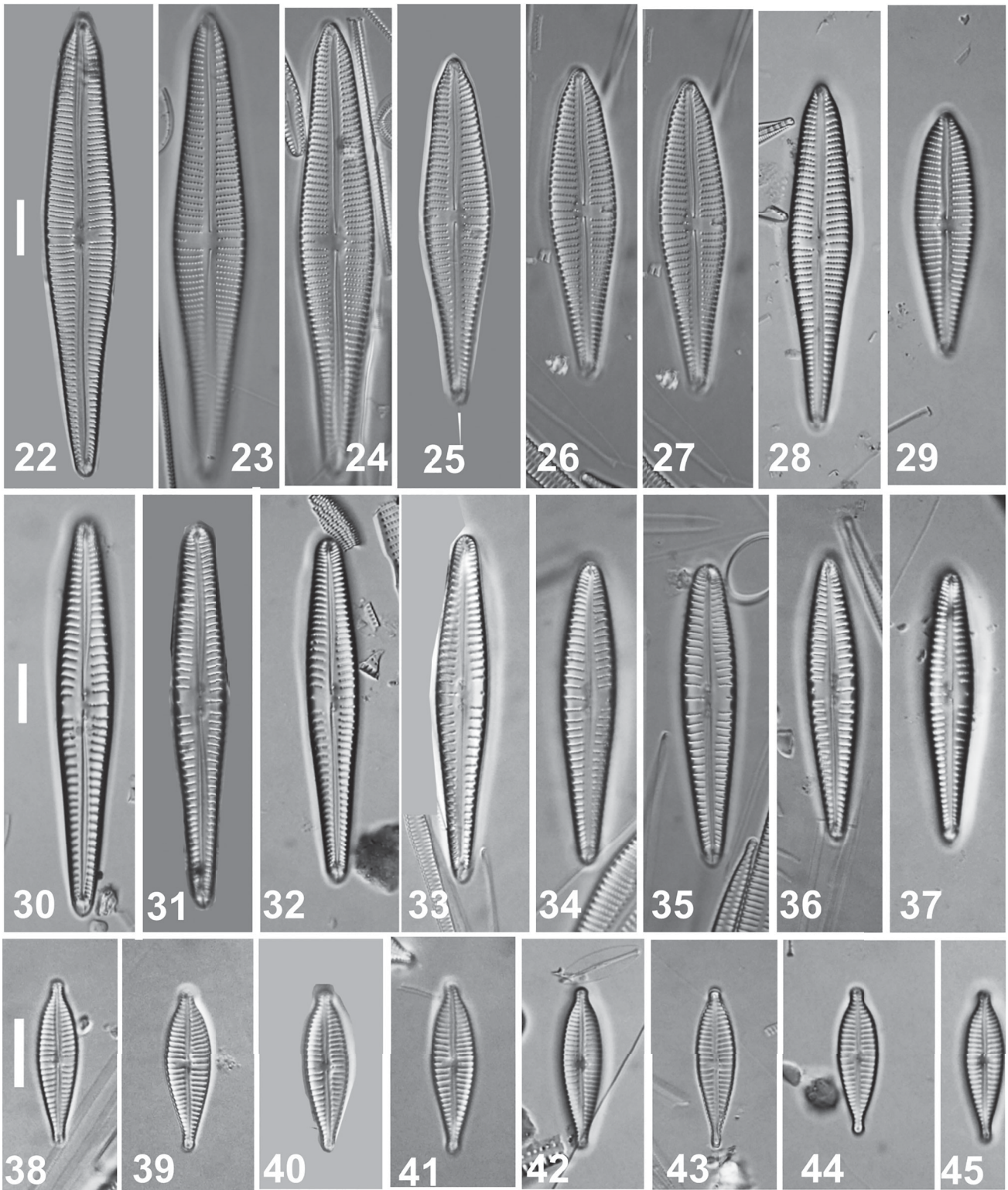


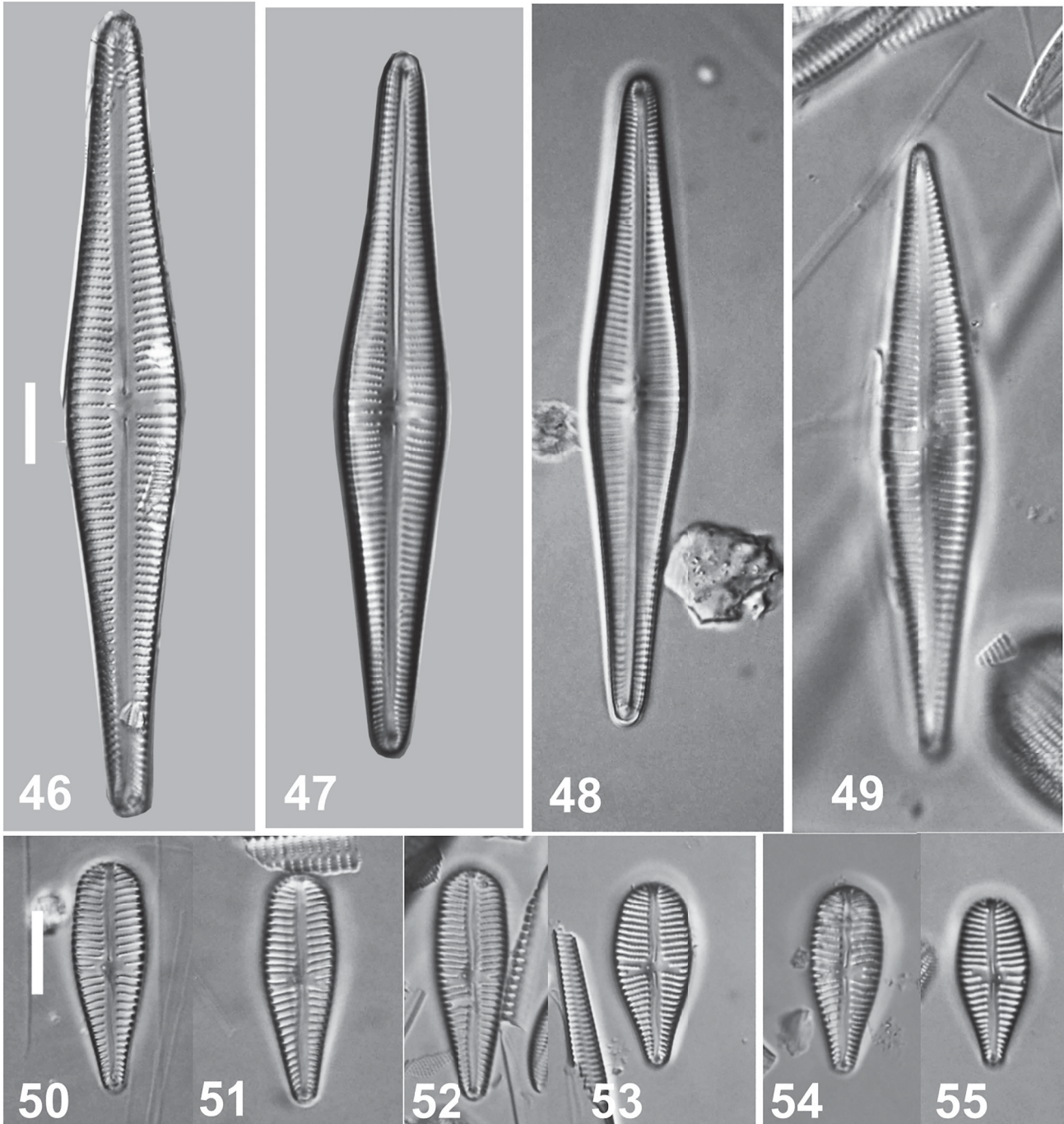
Fig. 1. a, b. Map showing location of Haqlan hot springs in Iraq. c. Photograph of the natural spring with sampling location on spring bank.



Figs 2–21. LM images of *Gomphonema* spp. Figs 2–7, *G. acuminatum*. Figs 8–15, *G. brockiae* sp. nov., Figs 16–21, *G. commutatum*. Scale bars: 10 μ m.



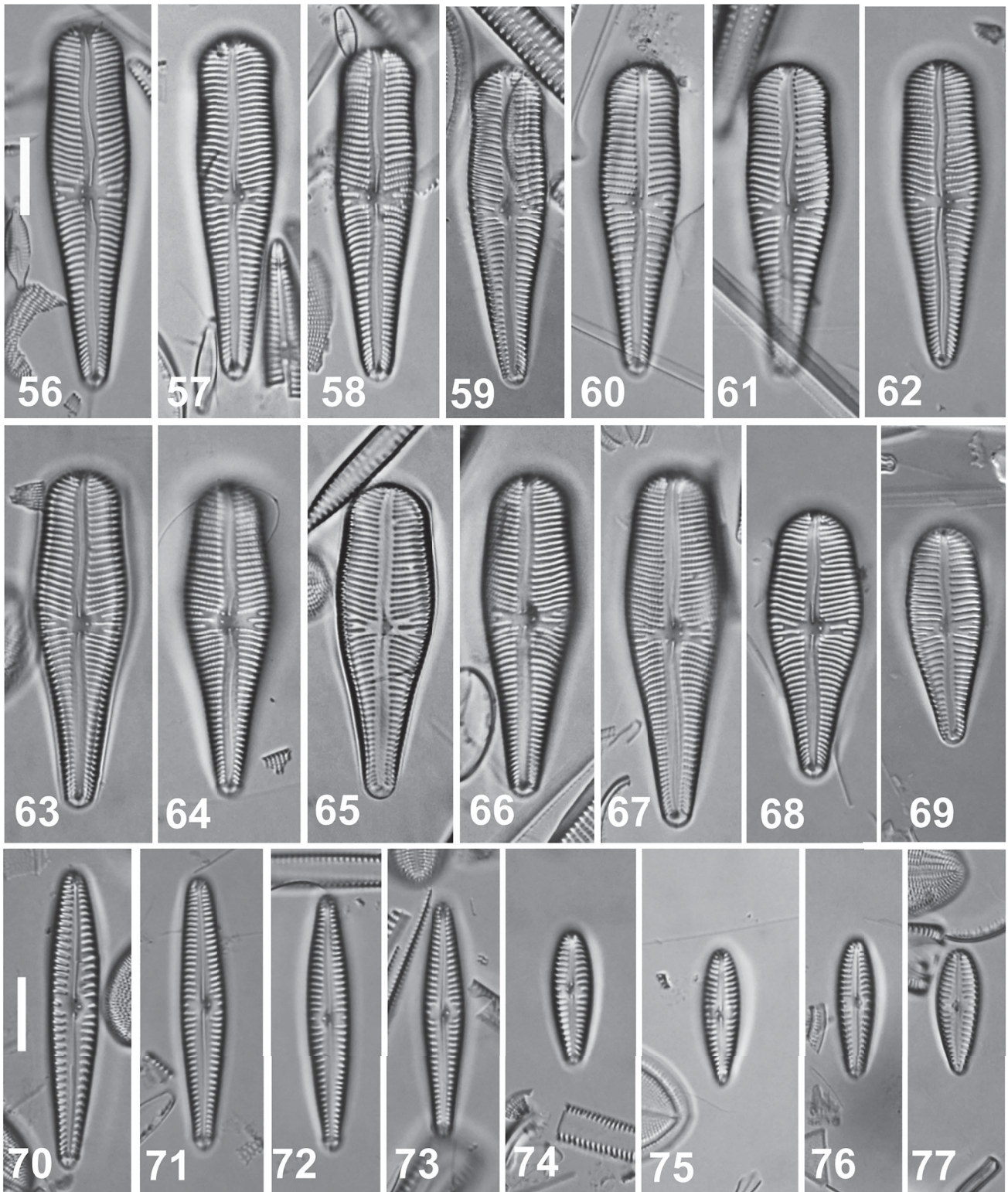
Figs 22–45. LM images of *Gomphonema* spp. Figs 22–29, *G. contraturris*. Figs 30–37, *G. dichotomum*. Figs 38–45, *G. exillissimum*. Scale bars: 10 μ m.



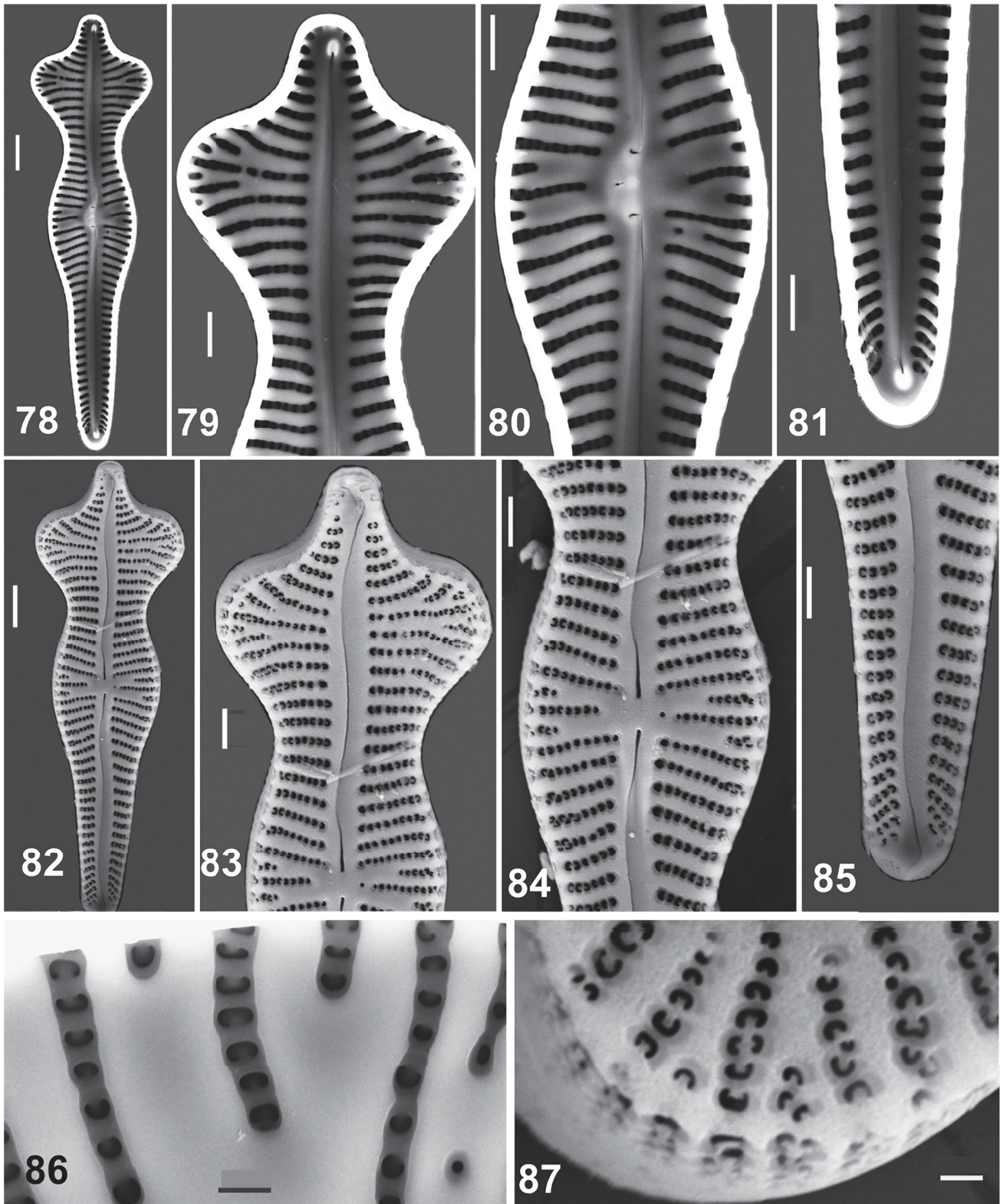
Figs 46–55. LM images of *Gomphonema* spp. Figs 46–49, *G. hadithaensis* sp. nov. Figs 50–55, *G. italicum*. Scale bars: 10 μ m.

raphe endings slightly expanded (Fig. 84), distal endings first deflected towards secondary (isolated pore side), then deflected on opposite side, extending onto the valve mantle to the other side (Fig. 83). At foot pole, raphe endings bisect apical pore field composed of small rounded pores (Fig. 85). External opening of isolated pore very small, rounded (Fig. 84). Striae at mid-valve and near head pole become bifurcate and biseriate near valve margin (Fig. 83).

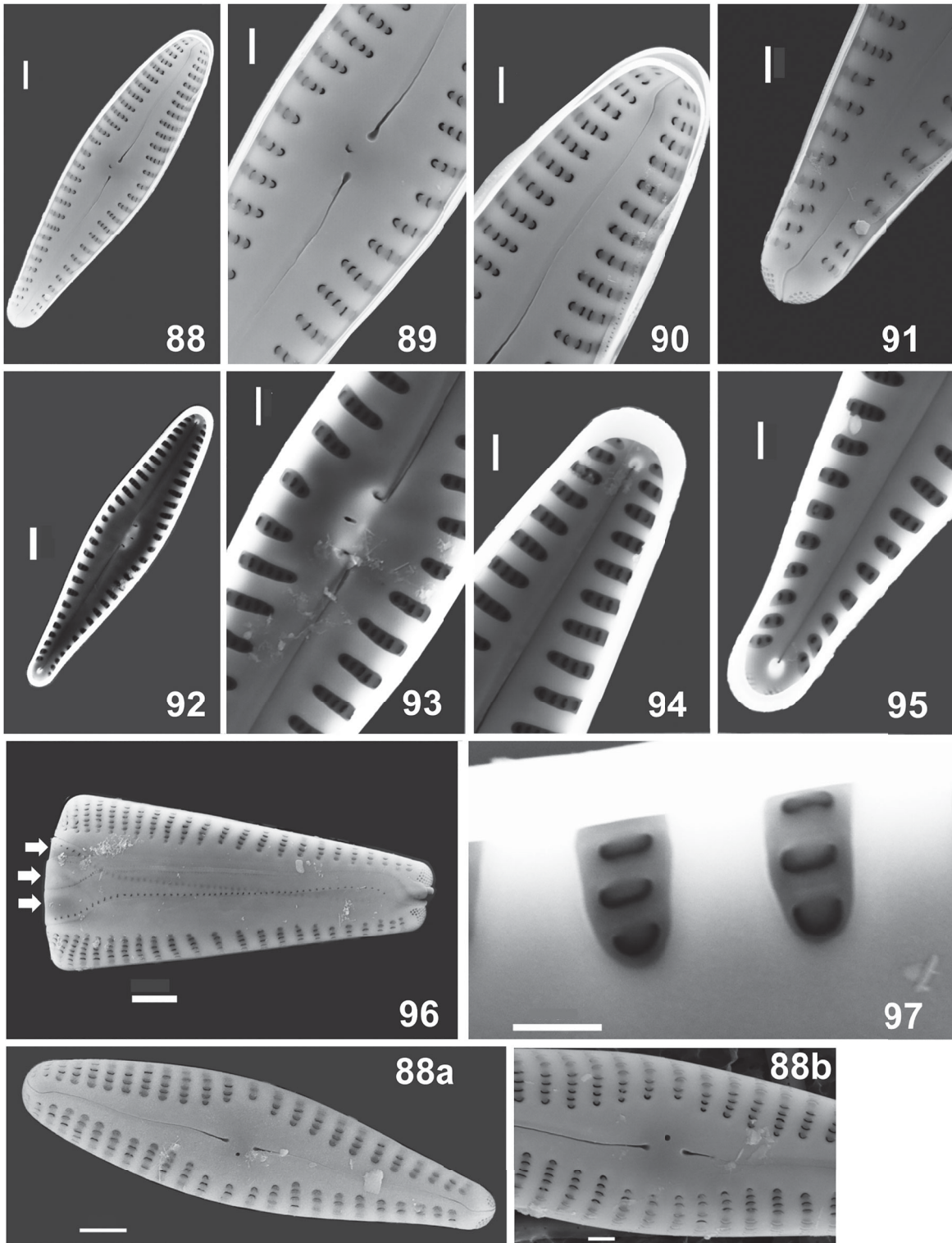
Areolae bordering the axial area are semi-rounded, become C-shaped towards valve margin (Fig. 87). Internally, proximal raphe ends hooked towards the isolated pore, distal endings terminate in small helictoglossae, shortly before apices (Fig. 79, 80). Isolated pore with slit-like opening (Fig. 80). Areolae sunk in narrow foraminal elongated pores separated by strongly silicified vimines (Fig. 86). Pore field well developed at base pole and located on valve



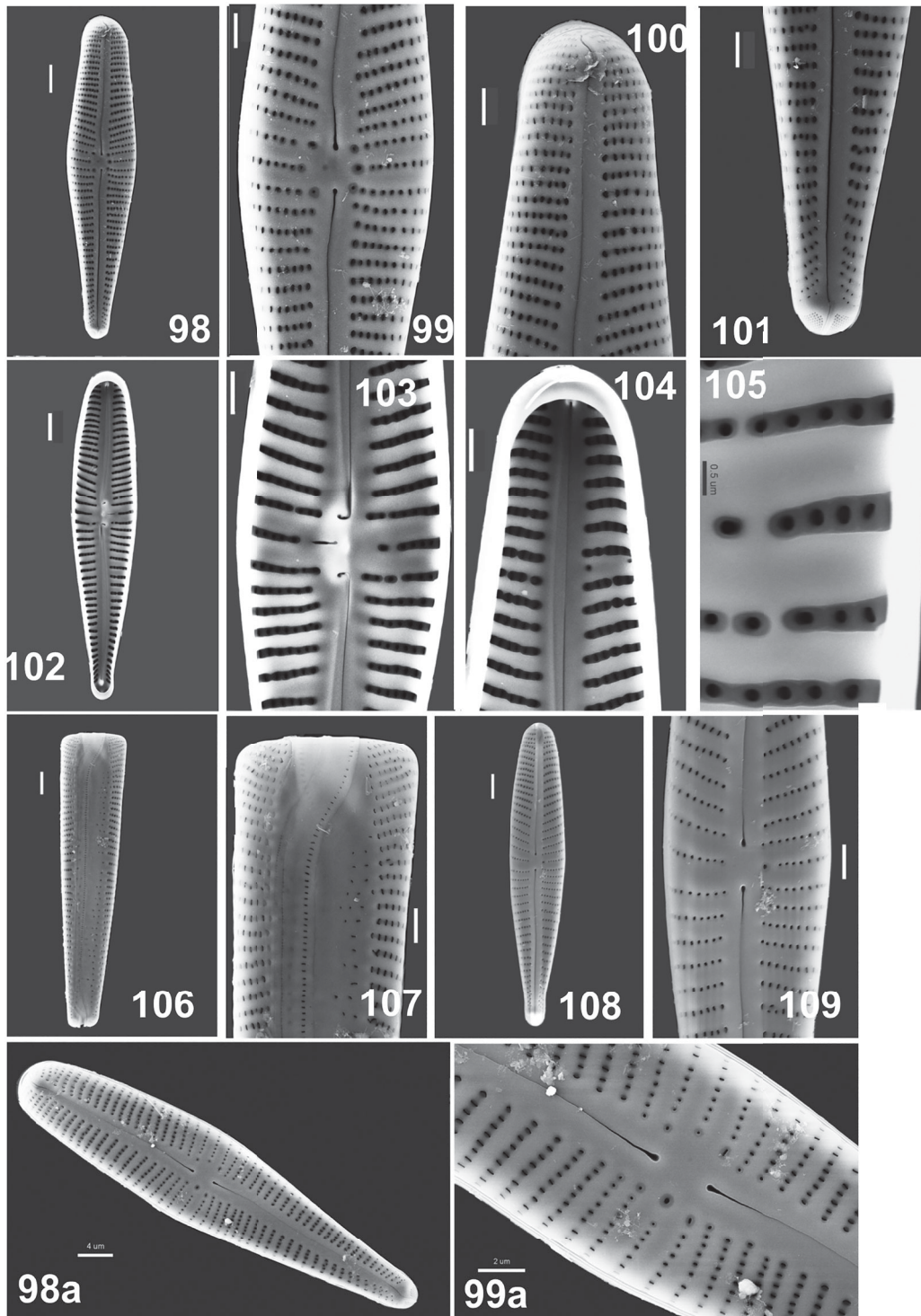
Figs 56–77. LM images of *Gomphonema* spp. Figs 56–69, *G. laticollum*. Figs 70–73, *G. procerum*. Figs 74–77, *G. pumilum*. Scale bars: 10 μ m.



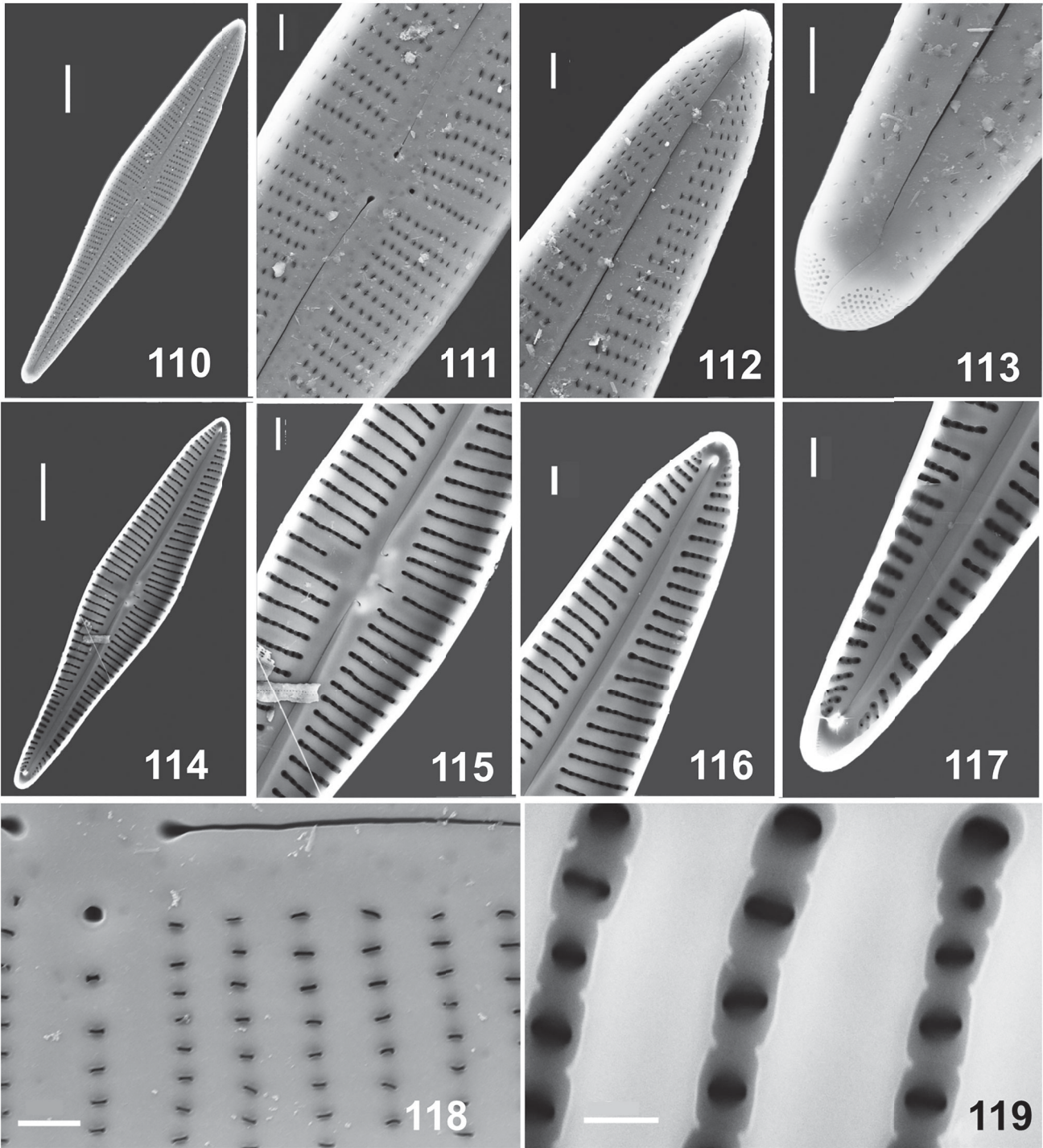
Figs 78–87. SEM images of *G. acuminatum*. Fig. 78. Valve internal side. Fig. 79. Upper half of the valve internal side. Marginal striae on the wider valve part below head pole are alternating short and long ones. Distal raphe ending in helictoglossa. Fig. 80. Mid-valve exhibiting central nodule, short and long striae and the curved raphe proximal endings. Fig. 81. Internal base pole. Fig. 82. Valve external side. Fig. 83. Enlarged upper half of the valve showing stria structure. Fig. 84. Mid-valve, the raphe proximal endings are expanded, the isolated pore is small and positioned at the end of a longer stria. Fig. 85. Valve base pole with the apical pore field. Fig. 86. Internal striae with narrow foramina and deep vimines, areolae C-shaped. Fig. 87. External C-shape areolae. Scale bars: Figs 78, 83: 4 μm . Figs 79–81, 83–85: 2 μm . Figs 86, 87: 0.5 μm .



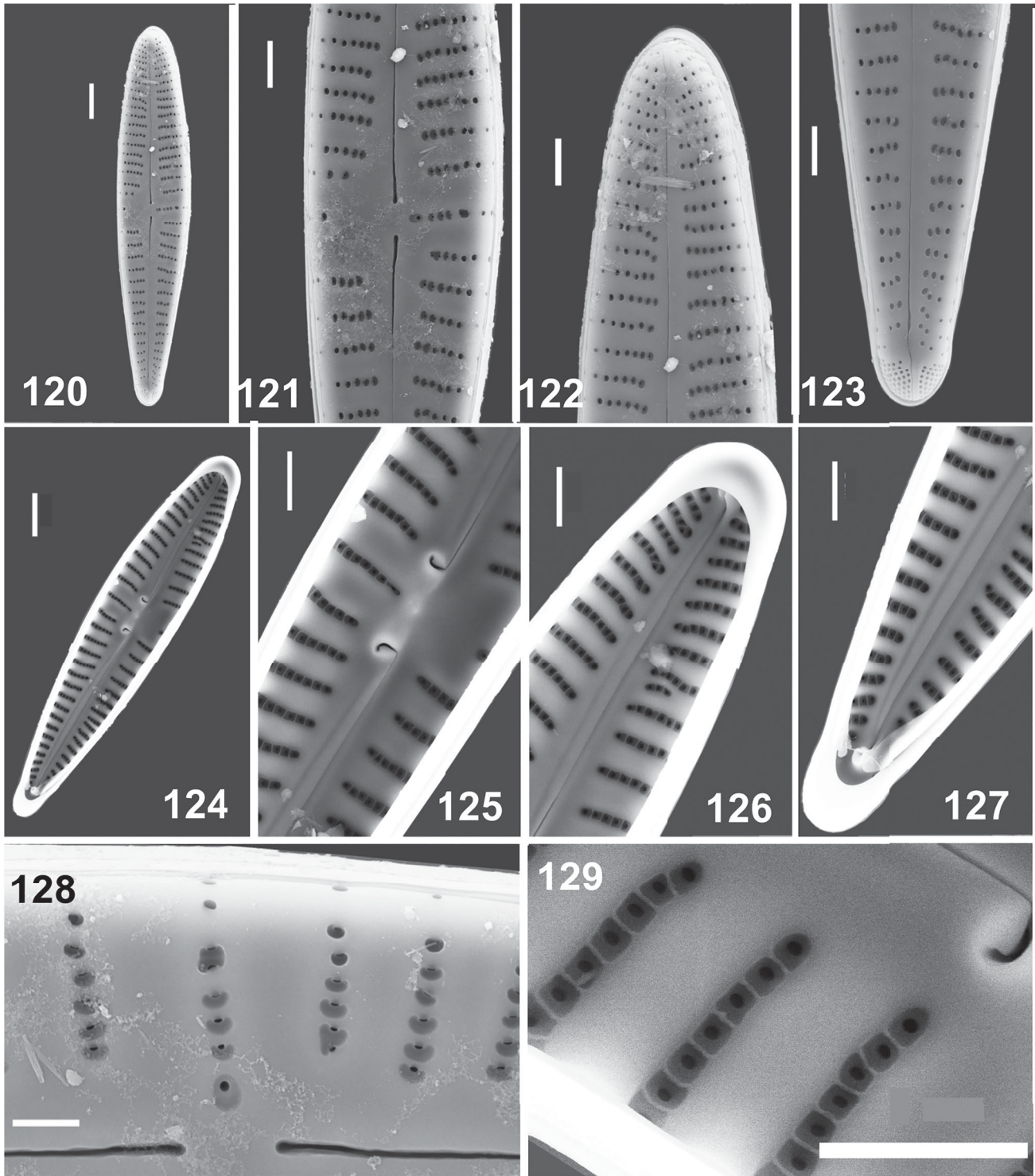
Figs 88–97. SEM images of *G. brockiae* sp. nov. Figs 88–91. External valve side. Figs 88, 88a, 88b. Valve outline of different cells. Fig. 89. Mid-valve showing short marginal striae, expanded raphe proximal endings and position of isolated pore. Fig. 90. Head pole with denser striae and weakly curved raphe distal ending. Fig. 91. Base pole with the apical pore field and raphe distal ending. Figs 92–95. Internal valve side. Fig. 93. Mid-valve with the hooked raphe proximal endings, the slit-like opening of the isolated pore and striae arranged in foramina separated by broad vimines. Fig. 95. Base pole with raphe distal ending in helictoglossa. Fig. 96. Frustule in girdle view showing perforated cingular bands and striae on valve mantle. Fig. 97. Internal areola shape. Scale bars: Figs 88, 88a, 92, 96: 2 μ m. Figs 88b, 89–91, 93–95: 1 μ m. Fig. 97: 0.5 μ m.



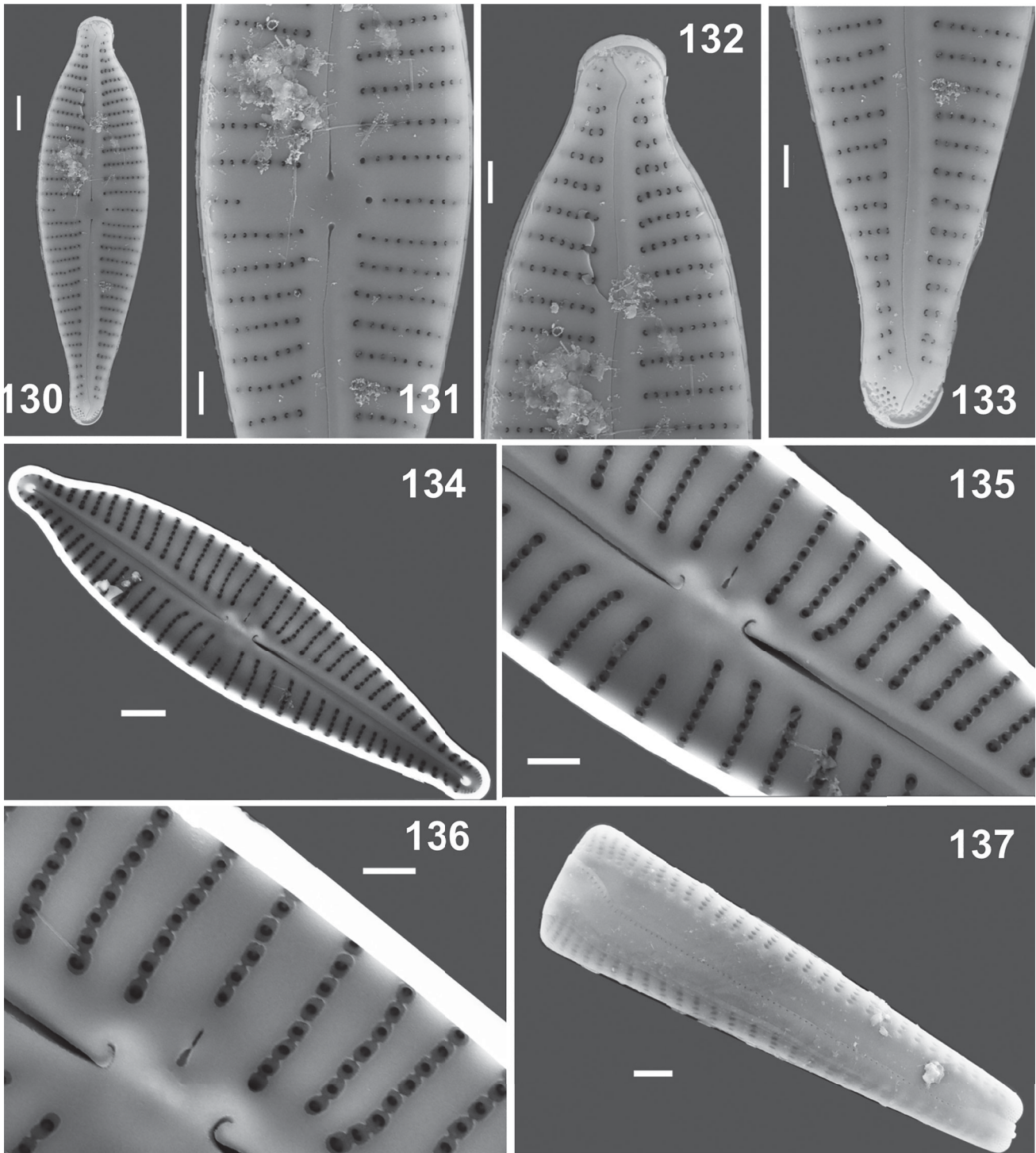
Figs 98–109. SEM images of *G. commutatum*. Figs 98–101. External valve side. Figs 99, 99a. Mid-valve, note the five isolated pore, only one opens into valve interior. Fig. 100. Head pole, striae more packed, raphe distal end curved towards the three isolated pores side. Fig. 101. Base pole, with the apical pore field bisected by distal raphe ending. Figs 102–105. Internal valve side. Fig. 103. Mid-valve, the curved raphe proximal endings and the narrow elongated isolated pore opening. Fig. 104. Head pole with narrow but well-developed pseudoseptum. Fig. 105. Internal rounded areola openings. Fig. 105. Frustule in girdle view. Fig. 107. Frustule head pole, note the discrete areolae on valve mantle, cingular bands with a single marginal row of elongated areolae. Fig. 109. External valve side of a specimen with a single isolated pore. Fig. 109. Enlarged mid-valve. Scale bars: Figs 98, 102, 106, 108: 4 μm. Figs 99–101, 103, 104, 107, 109: 2 μm. Fig. 107: 0.5 μm.



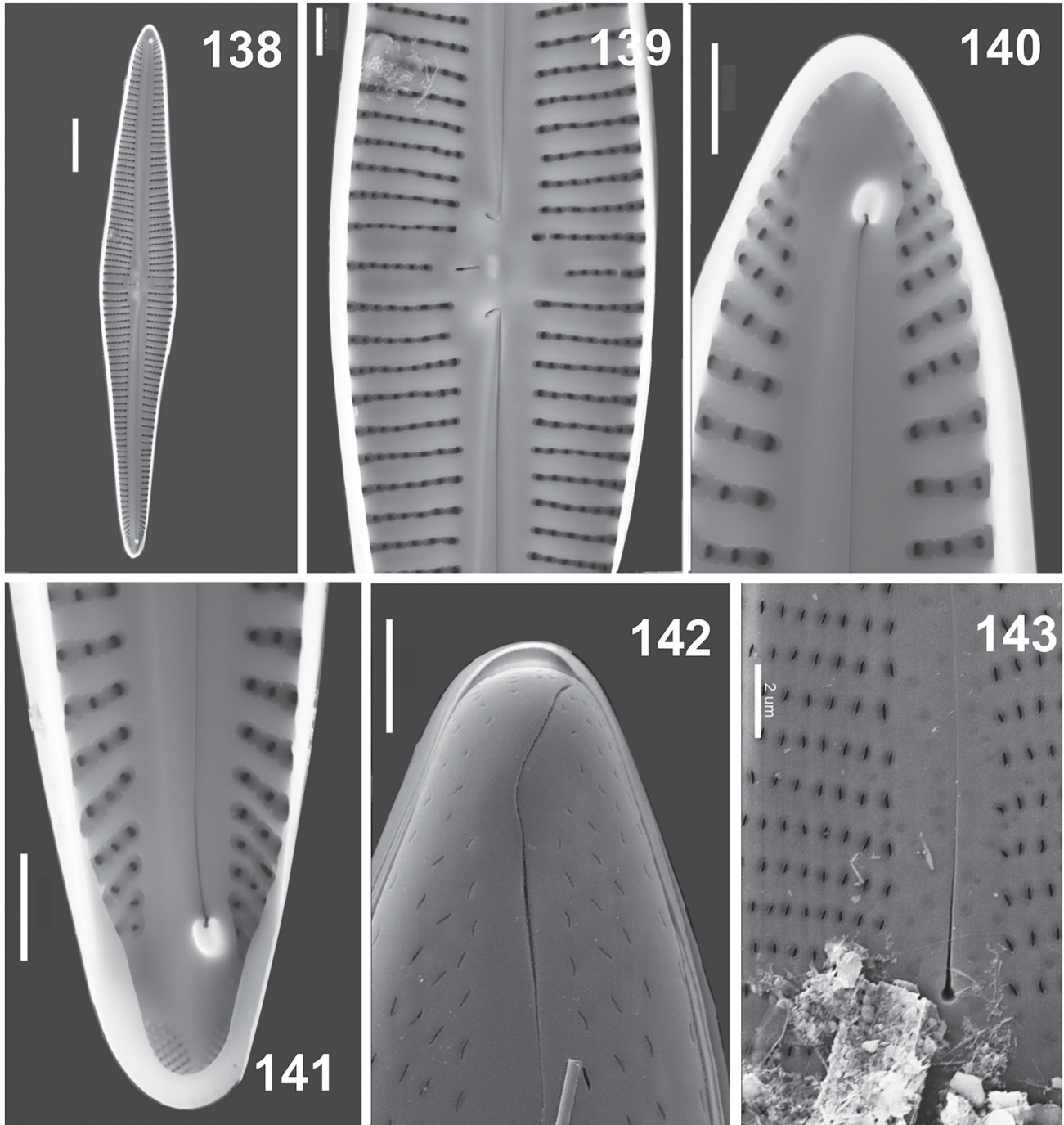
Figs 110–119. SEM images of *G. contraturris*. Figs 110–113. External valve side. Fig. 111. Mid-valve showing raphe proximal endings and position of the isolated pore. Fig. 112. Head pole with weakly curved raphe distal ending. Fig. 113. Base pole, note the stria arrangement and the apical pore field. Figs 114–117. Internal valve side. Fig. 115. Mid-valve showing curved raphe proximal endings and the elongated opening of the isolated pore. Fig. 116. Head pole with raphe distal ending in helictoglossa. Fig. 117. Base pole with narrow pseudoseptum. Fig. 118. External slit-like areolae. Fig. 119. Internal openings of areolae with irregular shapes. Scale bars: Figs 110, 114: 10 μm . Figs 111–113, 115–117: 2 μm . Fig. 118: 1 μm . Fig. 119: 0.5 μm .



Figs 120–129. SEM images of *G. dichotomum*. Figs 120–123. External valve side. Fig. 121. Mid-valve, note the very short stria on one side of the central area, the isolated pore positioned at the end of the long striae, areolae are sunk into lunar depressions. Fig. 122. Head pole showing the nearly straight raphe distal ending. Fig. 123. Base pole with a well-developed apical pore field. Figs 124–127. Internal valve side. Fig. 125. Mid-valve with curved raphe proximal endings. Note the isolated pore is not open on the inside. Fig. 127. Base pole with well-developed pseudoseptum. Fig. 128. External areola openings. Fig. 129. Internal areolae located in quadrangular depressions. Scale bars: Figs 120, 124: 4 μm . Figs 121–123, 125–127, 129: 2 μm . Fig. 128: 1 μm .



Figs 130–137. SEM images of *G. exillissimum*. Figs 130–133. External valve side. Fig. 131. Mid-valve showing raphe proximal endings, central area and isolated pore. Fig. 132: Head pole. Fig. 133. Slightly bent protracted base pole. Figs 134–136. Internal valve side. Fig. 135. Mid-valve showing curved raphe proximal endings and narrow elongated isolated pore opening. Fig. 135. Structure of areolae. Fig. 137. Frustule in girdle view. Scale bars: Figs 130, 134, 137: 2 μm. Figs 131–133, 135: 1 μm. Fig. 136: 0.5 μm.

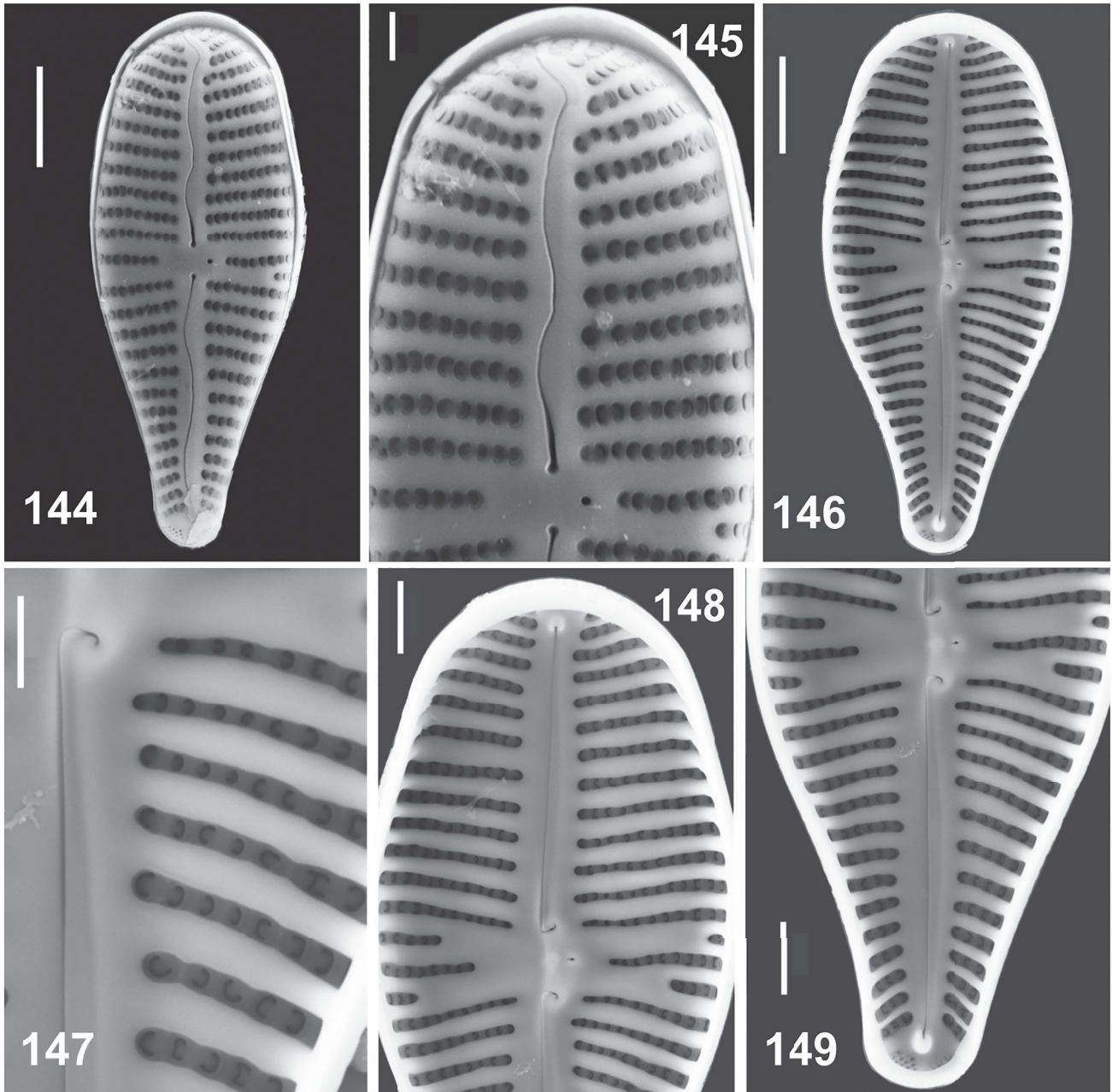


Figs 138–143. SEM images of *G. hadithaensis* sp. nov. Figs 138–142. Internal valve side. Fig. 139. Mid-valve exhibiting raphe proximal endings, and the linear narrow isolated pore opening. Fig. 140. Head pole, note the lateral raphe distal ending in helictoglossa and the linear openings of areolae. Fig. 141. Base pole showing the lateral raphe distal ending in helictoglossa, the apical pore field with very small poroids and the narrow pseudoseptum. Fig. 142. External head pole showing the laterally bent raphe distal ending and the irregular arrangement of the slit-like areolae. Fig. 143. External mid-valve. Scale bars: Fig. 138: 10 μm. Figs 139–143: 2 μm.

mantle (Fig. 85). A narrow pseudoseptum visible at the base pole (Fig. 81).

Remarks. *Gomphonema acuminatum* is a cosmopolitan species inhabiting fresh and brackish water with variable environmental preferences, from oligotrophic to eutrophic

waters (Reichardt 1999, Chudaev *et al.* 2014, Levkov *et al.* 2016, Abarca *et al.* 2020). Variation in valve morphology and stria structure were reported (Reichardt 1999, Kulikovskiy *et al.* 2015). Such variation has led to the description of several varieties. According to Abarca *et al.* (2020) based on microscopic observations and molecular



Figs 144–149. SEM images of *G. italicum*. Figs. 144–145. External valve side. Fig. 145. Head pole, note the strongly undulated raphe and curved raphe distal ending. Figs 146–149. Internal valve side. Fig. 147. Striae in narrow foramina separated by well-developed vimines. Fig. 148. Upper part of the valve showing raphe proximal endings and the isolated pore opening. Fig. 149. Lower part of the valve exhibiting raphe distal ending and the apical pore field. Scale bars: Figs 144, 146: 4 μm . Figs 145, 148, 149: 2 μm . Fig. 147: 1 μm .

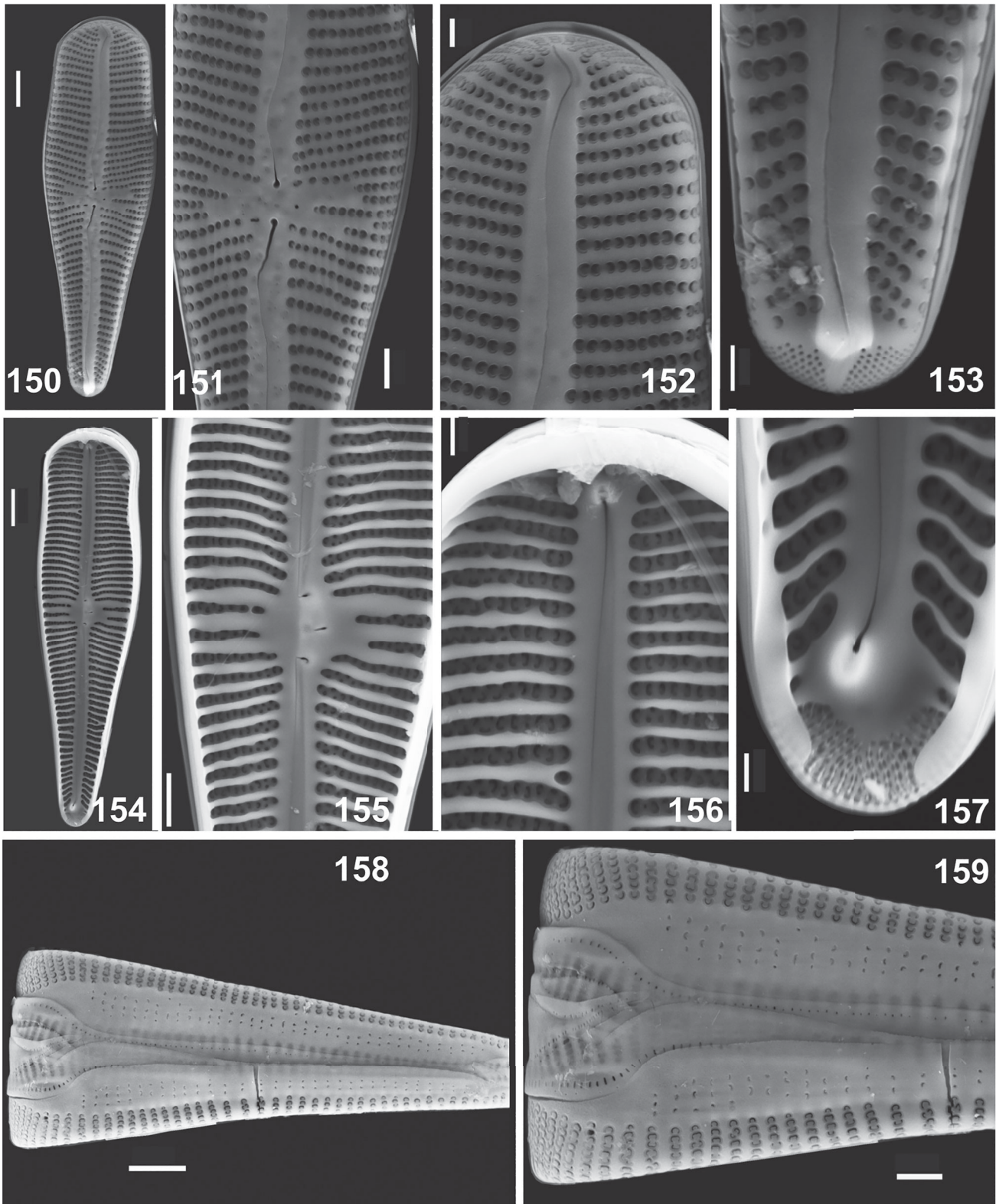
analyses of several strains of the *G. acuminatum* complex, many of these varieties may be conspecific. The areolae on the external valve face in the material from mid-Iraq are mostly semi rounded, becoming only C-shaped near the valve margin (Figs 83, 84), compared to completely C-shaped areolae in this species (Abarca et al. 2020, p. 138, figs 230–233, Levkov et al. 2016, p. 148, figs 6, 8). Such areola shape variation may be a result of the cleaning process. This species is widely distributed in Iraq and is one of

the common diatoms in the southern water systems of Iraq (Al-Handal & Al-Shaheen 2019).

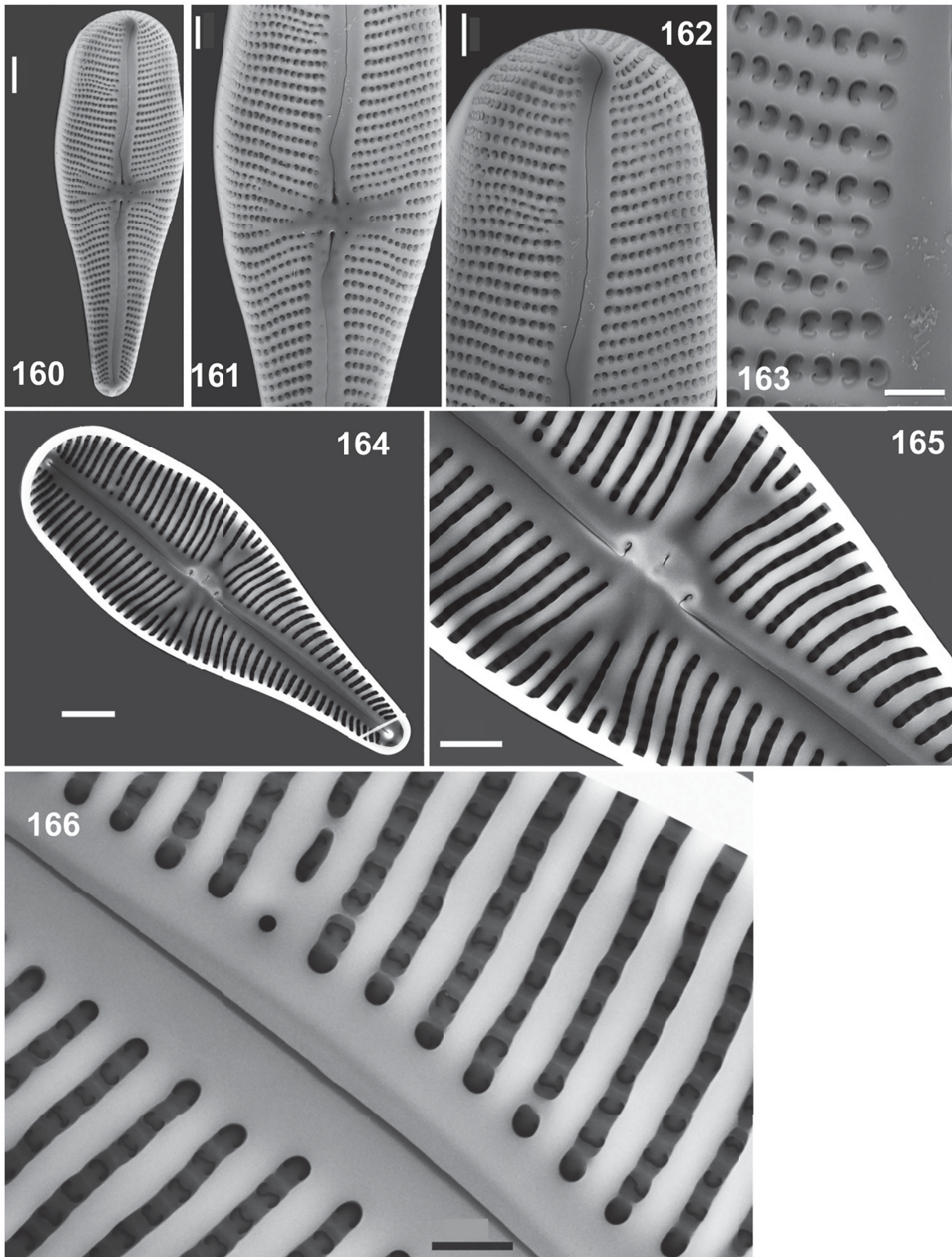
Occurrence and distribution. Frequent. Widely distributed in Iraq (Maulood et al. 2013).

***Gomphonema brockiae* Al-Handal, Levkov & Wulff sp. nov.** (Figs 8–15, 88–97)

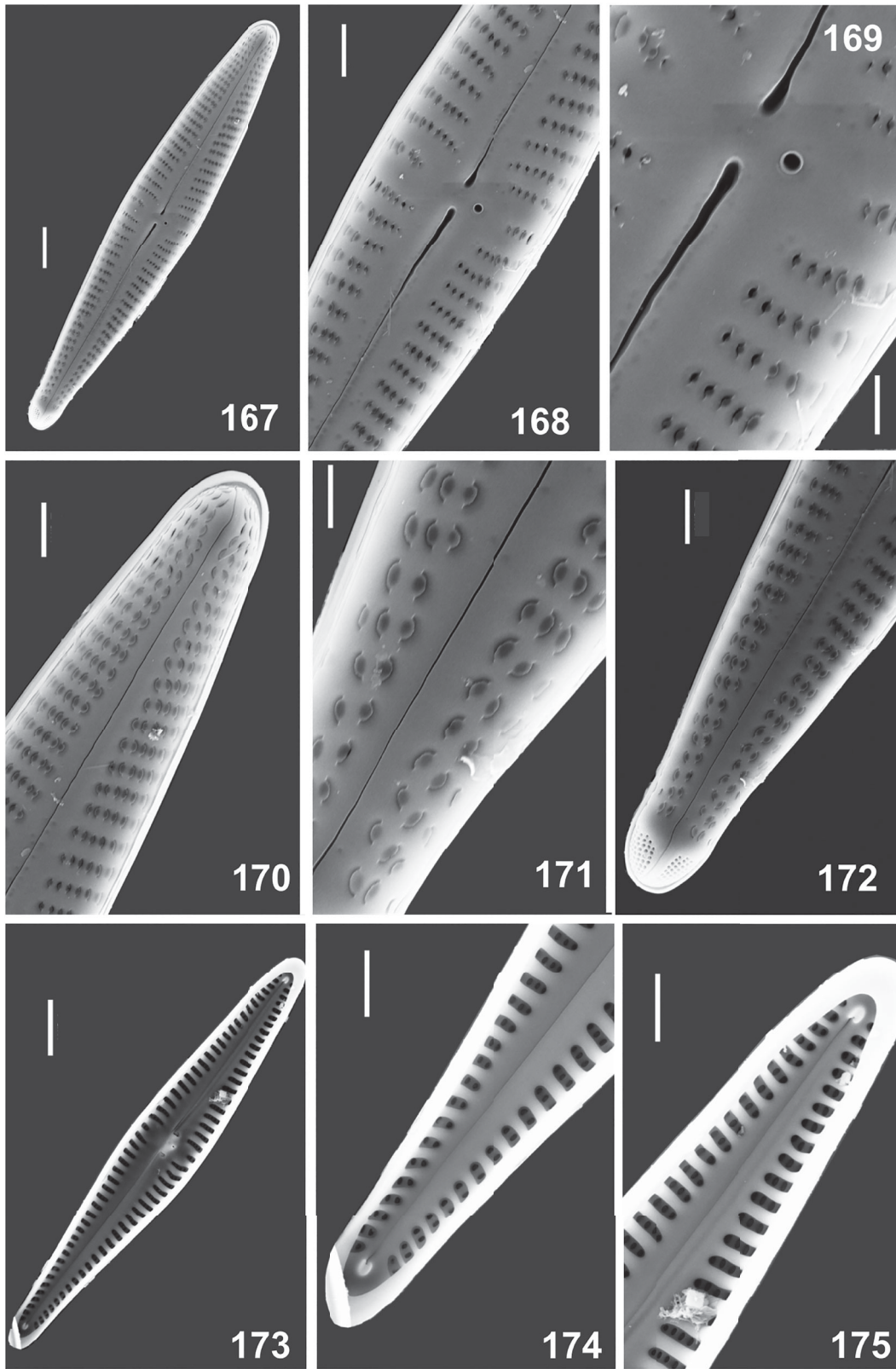
Description. LM observation (Figs 8–15): Valves clavate-lanceolate with rounded head pole and narrowly rounded,



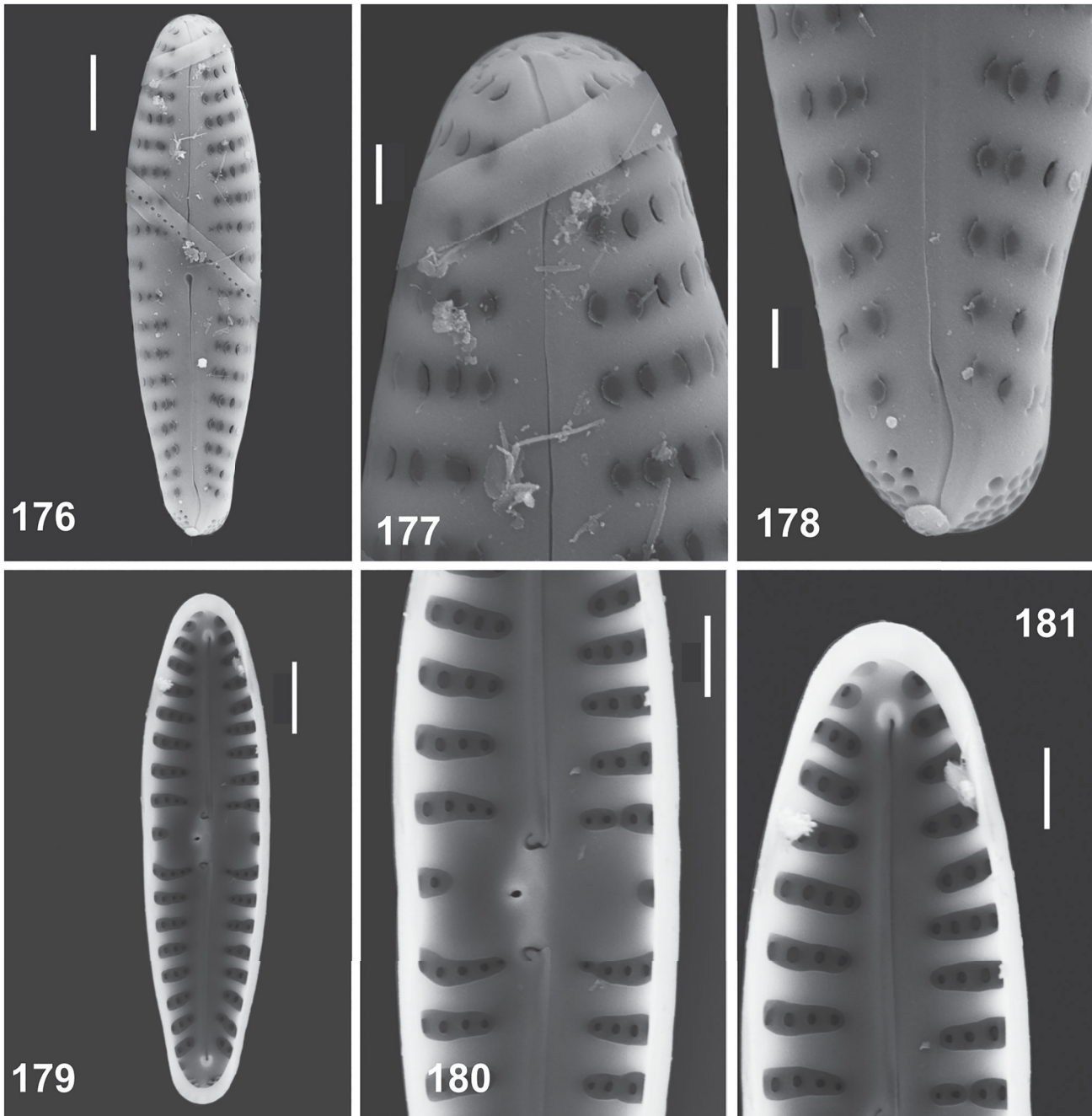
Figs 150–159. SEM images of *G. laticollum*. Figs 150–153. External valve side. Fig. 151. Mid-valve, with the bent raphe proximal endings and the small rounded isolated pore. Fig. 152. Head pole showing the curved raphe distal ending and areola structure which are deeply sunk C-shaped. Fig. 153. Base pole, note the curvature of raphe and the apical pore field formed of small, rounded areolae. Figs 154–157. Internal valve side. Fig. 155. Mid-valve showing central nodule, raphe proximal endings and isolated pore opening, the striae close to the axial area appear biseriate. Fig. 156. Head pole, note the deep foramina separated by strongly silicified and irregular vimines. Fig. 157. Base pole, note the deflected raphe distal ending, the structure of the apical pore field and the open narrow pseudoseptum. Fig. 158. Frustule in girdle view. Fig. 159. Enlarged upper part of the frustule showing cingular bands with discrete areolae on valve mantle. Scale bars: Figs 150, 154, 158: 4 μm . Figs 151, 155, 159: 2 μm , 152, 153, 156: 1 μm . Fig. 157: 0.5 μm .



Figs 160–166. SEM images of form 2 of *G. laticollum*. Figs 160–163. External valve side. Fig. 161. Mid-valve showing stria arrangement around the central area and raphe proximal endings. Fig. 162. Head pole, note the striae extend over apical mantle. Fig. 163. Structure of the C-shaped areolae. Figs 164–166. Internal valve side. Fig. 165. Mid-valve showing the hooked raphe proximal endings and the small slit opening of the isolated pore. Fig. 166. Narrow stria foramina separated by well-developed vimines. Scale bars: 160, 164: 4 μm. Figs 161, 162, 165: 2 μm. Figs 163, 166: 1 μm.



Figs 167–175. SEM images of *G. procerum*. Figs 167–172. External valve side. Fig. 168. Mid-valve. Fig. 169. Raphe proximal endings and the rounded isolated pore opening surrounded by silica ring. Fig. 170. Head pole. Fig. 171. Areola structure, C-shaped covered with silica flaps. Fig. 172. Base pole, note the nearly straight raphe distal ending bisecting a pore field. Figs 173–175. Internal valve side. Fig. 174. Base pole. Fig. 175. Head pole with pseudoseptum. Scale bars: Figs 167, 173: 4 μm . Figs. 168, 170, 172, 174, 175: 2 μm . Figs 169, 171: 1 μm .



Figs 176–181. SEM images of *G. pumilum*. Figs 176–178. External valve side. Fig. 177. Head pole. Fig. 178. Base pole, note the C-shaped areolae covered with silica flaps, the well-developed apical pore field formed of rounded areolae. Figs 179–181. Internal valve side. Fig. 180. Mid-valve showing curved raphe proximal endings and the small, rounded opening of the isolated pore, note the curvature of striae around the central area. Fig. 181. Head pole. Scale bars: Figs 176, 179: 2 μm . Figs 177, 178: 0.5 μm . Figs 180, 181: 1 μm .

slightly protracted foot pole. Valves 19–30 μm long, 5.5–6.5 μm wide with broadest part opposite to central area ($n = 36$). Axial area moderately broad, lanceolate, opens to wide rounded central area. Raphe slightly lateral, undulate, with tear-like elongated proximal endings. Striae parallel at mid-valve, slightly radiate towards poles, central striae shorter, 9–11 in 10 μm at mid-valve, 11–12 near the

poles. One isolated pore (stigma) located in the central area, close to raphe proximal endings.

SEM observation (Figs 88–97): Frustule in girdle view wedge-shaped (Fig. 96). Externally, raphe branches undulated (Figs 88–90). Proximal raphe endings straight, expanded, tear drop-shaped (Fig. 89). Distal raphe endings weakly hooked and extended to valve mantle (Figs 90, 91).

Well-developed apical pore field located at foot pole and extends to mantle, composed of small, rounded areolae, bisected by distal raphe end (Fig. 91). Striae uniseriate, extending onto mantle (Figs 90, 96). Areolae adjacent to axial area C-shaped, becoming apical slits towards valve margin (Fig. 90). Areolae sunk into valve face in elongated depressions separated by well-developed ribs (Fig. 89, 90). Isolated pore small, rounded (Figs 88a, 88b) or curved (Fig. 89), located distantly from central stria and laterally between raphe proximal endings (Fig. 89). Three open bands overlapping each other with marginal apical row of small poroids (Fig. 96, arrows). Internally, raphe proximal endings hooked on slightly elevated central nodule (Fig. 93). Raphe distal endings terminate on helictoglossae, shortly before valve poles (Figs 94, 95). Striae weakly radiate around central nodule (Fig. 93), parallel towards the head pole (Fig. 94). Areolae arranged in foraminal rows, C-shaped to slightly elongated openings (Fig. 97). Isolated pore opening transapically elongated (Fig. 93). Weakly developed pseudoseptum located at both poles (Figs 94, 95).

Holotype. Permanent slide containing valves of *G. brockiae* sp. nov. is deposited in the Botanischer Garten und Botanischer Museum (BGBM), Berlin, Germany under accession B 40 0045805. Phycobank registration number: <http://phycobank.org/104938>. Holotype illustrated in Figs 8–15.

Type locality. Heqlan springs (34°05'27" N, 42°21'57" E), Euphrates River, Iraq.

Etymology. The epithet is in honour of Dr Elisabet Brock of the Tjärnö Marine Laboratory (TMBL), University of Gothenburg, because her invaluable contributions to spreading algal knowledge among students and teachers have made a significant impact on science education.

Occurrence and distribution. Frequent in all samples.

Gomphonema commutatum Grunow *sensu lato* (Figs 16–21, 98–109)

Krammer & Lange-Bertalot (1986), p. 367, pl. 163, figs 1–12 (as *G. clavatum* Ehrenberg); Thomas et al. (2009), p. 216, figs 65–67.

Morphology. Valves heteropolar, clavate to rhombic-lanceolate, with broadly rounded head pole and narrowly rounded, weakly protracted foot pole. Valves 48–52 µm long, 9.0–11.0 µm wide with widest part at mid-valve. Axial area linear, narrow. Central area irregular, rounded, elliptical to almost absent. Raphe lateral, undulated. Raphe proximal endings elongated, straight, drop-like. Isolated pore very close to median stria. Raphe distal endings weakly deflect towards pore-bearing side, and then deflected to opposite side, extending onto valve mantle. Striae weakly radiate throughout, 10–12 in 10 µm at mid-valve, 12–14 in 10 µm towards head pole. In the SEM,

externally, one isolated pore present in the central area (Figs 98, 99). Areolae near proximal raphe endings slightly larger, giving impression of isolated pores (Figs 99, 99a). At foot pole, raphe bisect a pore field composed of small, rounded areolae (Fig. 101). Areolae rounded to short slit-like, areolae in the row adjacent to axial area are C-shaped (Figs 99, 100). Internally, raphe lateral with proximal endings hooked on raised central nodule (Fig. 103). Distal raphe endings terminate in helictoglossae (Figs 102, 104). Isolated pore opening very narrow, slit-like (Fig. 103). Striae separated by strongly silicified vimines. Areolae sunk in narrow foraminal rows (Fig. 105). Small pseudosepta on both valve poles (Fig. 102).

Remarks. *Gomphonema commutatum* is a variable species with varying valve outline from a clavate form to lanceolate with tumid mid-valve, which lead to the description of several taxa regarded now as synonyms, including *G. clavatum* Ehrenberg, *G. longipes* Ehrenberg, *G. mexicanum* Grunow, *G. montanum* Schumann, *G. montanum* var. *commutatum* (Grunow) Grunow, *G. subclavatum* var. *commutatum* (Grunow) Mayer, *G. musela* Ehrenberg and *G. obliqua* (Grunow) O. Muller. The population from Haqlan hot springs has rounded external areola openings, compared to typical C-like openings in *G. commutatum*. However, such areola shape might be a result of corrosion during the cleaning process.

Occurrence and distribution. Frequent. Not recorded previously from Iraq.

Gomphonema contraturris Lange-Bertalot & E.Reichardt (Figs 22–29, 110–119).

Lange-Bertalot (1993), p. 57, pl. 78, figs 2–9, pl. 79, figs 1–5.

Morphology. Valves heteropolar, clavate-lanceolate with widest part at mid-valve. Head pole cuneate-apiculate, terminating in angular apex, foot pole acutely rounded. Valves 34–90 µm long, 13.0–16.0 µm wide. Axial area linear, slightly widens into unilaterally expanded central area, formed by shortening of central stria. Raphe, slightly lateral and weakly undulated. Striae weakly parallel at mid-valve, strongly radiate near poles, 10–11 in 10 µm at mid-valve, 11–13 in 10 µm towards poles. In the SEM, externally, proximal raphe endings straight, distant and drop-like (Fig. 111). Raphe distal endings slightly bent towards the isolated pore side and extend to valve mantle (Figs 112, 113). Isolated pore small, rounded (Fig. 111). At foot pole, raphe ending bisects a well-developed pore field formed of rounded pores (Fig. 113). Areola foramina appear as short apical slits, slightly sunk into valve face (Fig. 118). Internally, proximal raphe endings hooked, slightly raised on elevated central nodule (Fig. 115). Raphe distal endings terminate in helictoglossae, shortly before apices (Figs 116, 117). Isolated pore opening

very narrow, transapically elongated (Fig. 115). Areola openings elliptical to rounded (Fig. 119).

Occurrence and distribution. Frequent in all samples. Not recorded previously from Iraq.

Gomphonema dichotomum Kützing *sensu lato* (Figs 30–37, 120–129)

Reichardt & Lange-Bertalot (1991), pl. 1, figs 1–14, Reichardt (2018), pl. 320, fig. 23.

Morphology. Valves slightly heteropolar, lanceolate to linear-lanceolate with narrowly rounded head pole and slightly protracted rounded foot pole. Valves 48–63 µm long, 8.0–9.0 µm wide, with broader part near mid-valve. Axial area narrow, gradually widens towards asymmetrical, laterally expanded central area, formed by a short stria on one side of the central area. Raphe slightly lateral, filiform, weakly undulated. Raphe proximal endings expanded, slightly deflected towards the isolated pore. Striae weakly radiate throughout, 7–9 in 10 µm at mid-valve, 11–13 towards poles. In the SEM, externally, proximal raphe endings, slightly expanded and deflected towards the isolated pore (Fig. 121). Distal raphe endings straight and terminate on valve mantle (Fig. 122), bisecting a pore field at foot pole (Fig. 123). Apical pore field formed of rounded porelli. One strongly shortened central stria composed of 1–2 areolae on the side opposite to the isolated pore (primary side) (Figs 121, 125). Isolated pore with rounded external opening, slightly sunk into valve face, located at the end of a long stria (Fig. 121). Areolae individually slightly sunk into valve face, formed of either small, rounded openings, short slits or C-shaped, positioned in lunar depressions (Figs 121, 128). Internally, proximal raphe endings hooked, distal endings terminate in elevated helictoglossae. Isolated pore does not open internally (Fig. 125). Striae arranged in narrow foraminal rows, sunk into quadrangular depressions (Fig. 129). Areola openings small, rounded to elliptical (Figs 125, 129). Valves with short pseudosepta at both poles (Fig. 124).

Remarks. *Gomphonema dichotomum* observed in our material appears similar to *G. amoenum* (Levkov et al. 2016, p. 25, figs 83: 1–28, 84: 1–9) in having a stria composed of a single areola on one side of the central area. However, the valves of *G. amoenum* are less clavate with more elongated headpoles. Striae are denser (11–15 at mid-valve and 15–18 in 10 µm near the poles) and the areolae are more packed. Krammer & Lange-Bertalot (1986, p. 370) considered *G. dichotomum* as a synonym to *G. angustum* C. Agardh, but the list of synonyms indicate a wide variation of valve outline of this species. Later, Reichardt & Lange-Bertalot (1991), considered it as a separate species belonging to the *G. angustum-dichotomum-intricatum-vibrio* species complex.

Population of *G. dichotomum* from Haqlan hot spring is morphologically similar to *G. dichotomum sensu stricto*,

but differences can be noticed in the shape of the external areola openings. According to Reichardt & Lange-Bertalot (1991, fig. 1: 13), the external areola openings in *G. dichotomum* are typically C-like, while in the population from Haqlan hot spring they have round foramina. Also, the proximal raphe endings are straight, compared to teardrop-shaped in the type material. However, all other morphometrical and ultrastructural features are comparable.

Occurrence and distribution. Frequent in all samples. Not recorded previously from Iraq.

Gomphonema exilissimum (Grunow) Lange-Bertalot & E. Reichardt (Figs 38–45, 130–137)

Lange-Bertalot & Metzeltin (1996), p. 70, pl. 62, figs 23–27, Levkov et al. (2016), pl. 127, figs 1–33, pl. 128, figs 1–41, pl. 129, figs 1–7, pl. 131, figs 26–47.

Morphology. Valves heteropolar, linear lanceolate to narrowly elliptic, with subcapitate to slightly rostrate rounded poles. Foot pole in some specimens slightly deflected (Fig. 39). Valves 19–20 µm long, 5.5–7.0 µm wide. Axial area linear, very narrow. Central area small, irregular, may become unilaterally expanded due to a short stria on one side. Raphe filiform, slightly lateral, undulated. Striae weakly radiate throughout, 11–12 in 10 µm at mid-valve, 13–14 towards the poles. In the SEM, externally, proximal raphe endings expanded, drop-like and slightly deflected towards the isolated pore (Figs 130, 131). Distal raphe endings first curved towards isolated pore side and extend on mantle (Fig. 132). Foot pole raphe ending bisects a well-developed apical pore field formed of rounded porelli, different from the rest of areolae (Fig. 133). Areolae small, slightly sunk into valve face, with variable shape (Figs 131, 132). Isolated pore small, rounded, located at the end of a long central stria (Fig. 131). Internally, raphe straight, proximal endings strongly hooked, distal endings terminate in helictoglossae (Figs 134, 135). Areolae C-shaped to irregular, surrounded by thin silica thickenings and arranged in shallow foramina (Figs 135, 136). Isolated pore opening slit-like, elongated (Fig. 136). Pseudosepta absent at both poles (Fig. 134).

Remarks. This species was originally described as a variety of *G. parvulum* (*G. parvulum* var. *exilissimum* Grunow), and later erected as a distinct species by Lange-Bertalot & Reichardt (in Lange-Bertalot & Metzeltin 1996). The characterization of *G. exilissimum* by Jüttner et al. (2013) was mostly based on valve length-width ratio which does not seem to be a good feature due to the varying ratio and valve outline of the species. Levkov et al. (2016) encountered different valve morphologies such as valve outline and pole shapes, which led them to consider these as different morphotypes of the species (Levkov et al. 2016, pl. 128, figs 1–41, pl. 129, figs 1–7, pl. 131, figs 26–47). The observed specimens appeared with narrowly elliptic valves

and a headpole more subcapitate than the basal pole, which match the description of *G. exilissimum*.

Occurrence and distribution. Frequent. Not recorded previously from Iraq.

***Gomphonema hadithaensis* Al-Handal, Levkov & H. Abdullah sp. nov.** (Figs 46–49, 138–143)

Description. LM observation (Figs 46–49): Valves isopolar to slightly heteropolar, rhombic lanceolate with largest valve width at mid-valve. Head and foot poles acutely rounded. Valves 85–102 µm long, 13.0–15.0 µm wide. Axial area linear, slightly wide. Central area small, irregular, laterally dilated towards a short stria, opposite to isolated pore. Raphe filiform, slightly undulated, lateral. Proximal raphe ends small, drop-like, weakly deflected to isolated pore side. Striae parallel at mid-valve, convergent towards poles, 7–9 in 10 µm at mid-valve, 13–15 in 10 µm towards poles. Areolae visible in LM.

SEM observation (Figs 138–143): Internally, proximal raphe ends hooked (Fig. 139). Distal raphe endings at both poles deflected to the side opposite to isolated pore, terminated in obliquely positioned helictoglossae (Figs 140, 141). Isolated pore opening narrowly elongated (Fig. 139). Striae arranged in very narrow foraminal rows. Areolae mostly rounded or slit-like (Figs 140, 141). Apical pore field on the foot pole formed of very small porelli, different in shape than the rest of the valve (Fig. 141). Externally, distal raphe endings deflected to the side opposite to isolated pore, extending onto mantle (Fig. 142). Striae formed of slit-like areolae, apically arranged at mid-valve and oblique towards poles (Figs 142, 143). A weakly developed pseudoseptum at foot pole (Fig. 141).

Holotype. Permanent slide containing valves of *G. hadithaensis* sp. nov. is deposited in the Botanischer Garten und Botanischer Museum (BGBM), Berlin, Germany under accession B 40 0045806. Phycobank registration number: <http://phycobank.org/104939>. Holotype illustrated in Fig. 46.

Type locality. Heqlan springs (34°05'27" N, 42°21'57" E), Euphrates River, Iraq.

Etymology. The epithet refers to the locality where this species was found (Haditha Town, Iraq).

Occurrence and distribution. Very rare, encountered only in one sample.

***Gomphonema italicum* Kützing** (Figs 50–55, 144–149)

Reichardt (2001), p. 202, pl. 6: 1–24; pl. 7: 1–6, pl. 14: 7–13, Levkov *et al.* (2016), pl. 15, figs 1–16, pl. 23, figs 6–8.

Morphology. Valves broadly clavate with broadly rounded to truncate head pole and weakly acuminate rounded base pole. Valves 18–22 µm long, 8.0–9.5 µm wide at broadest middle part. Axial area linear and narrow. Central

area small, irregular, bordered by 1–3 irregularly shortened striae. One isolated pore present in the central area at end of longest central stria. Raphe undulated, lateral. Proximal raphe endings expanded, tear-drop-shaped. Striae weakly radiate throughout, 12–15 in 10 µm. In the SEM, externally, raphe strongly undulated (Fig. 144). Proximal raphe endings deflected towards isolated pore (Fig. 145). Distal raphe endings at head pole first curved towards isolated pore side, then bent to opposite side on mantle (Figs 144, 145). At base pole, raphe end bisects apical pore field, formed of small, rounded porelli (Fig. 144). Areolae C-shaped, slightly sunk into valve face (Fig. 145). Internally, proximal raphe endings hooked (Fig. 146). Striae located in narrow foraminal rows between strongly silicified vimines, (Figs 148, 149). Internal openings of areolae C-shaped (Fig. 147). Narrow pseudosepta present at both poles (Figs 148, 149).

Remarks. The observed specimens of *G. italicum* may represent the smallest valve dimensions reported for this species. In this study, the largest valve length did not exceed 22 µm, whereas valves up to 60 µm long have been documented in the literature (Medeiros *et al.* 2018).

Occurrence and distribution. Rare. Previously recorded from southern Iraq (Al-Handal & Al-Shaheen, 2019).

***Gomphonema laticollum* E.Reichardt** (Figs 56–69, 150–166)

Reichardt (2001), p. 199, figs 5: 1–14, Levkov *et al.* (2016), p. 74, pl. 22, figs 1–15, pl. 23, figs 1–5, pl. 24, figs 1–25, pl. 25, figs 1–8, pl. 26, figs 13–19.

Morphology. Valves clavate, heteropolar, slightly tumid at mid-valve and weakly constricted towards both poles. Head pole broadly rounded to truncate, foot pole narrowly rounded. Valves 28–50 µm long, 10.0–13.0 µm wide. Axial area linear, narrow, slightly widened between central area and poles. Central area small, irregular, located below widest part of the valve. One isolated pore present in the central area, located at the end of long central stria. Raphe lateral, undulated, proximal raphe endings deflected towards isolated pore. Striae strongly radiate at mid-valve and weakly radiate towards poles, 11–13 in 10 µm at mid-valve, 13–14 near poles. Striae bordering central area alternate between short and long one. In the SEM, externally, proximal raphe endings expanded (Figs 155, 165). Distal raphe endings first curved towards isolated pore, then deflected on the opposite side, extending onto valve mantle (Figs 152, 162). At foot pole, raphe distal end bisects a well-developed apical pore field formed of small, rounded porelli (Fig. 153). Areolae C-shaped, sunk into rounded depressions (Figs 152, 162, 163). Occasionally, few isolated areolae do not penetrate internally giving impression of isolated pores in the central area (Fig. 161). Internally, proximal raphe endings hooked (Figs 155, 165). Distal raphe endings terminate in helictoglossae (Fig. 164).

Raphe end at foot pole deflected to the side opposite to isolated pore (Fig. 157). Striae partly biserial adjacent to axial area at mid-valve and towards margin near the poles (Figs 155, 156). Areola C-shaped, arranged in relatively deep and narrow foraminal rows separated by strongly silicified vimines (Figs 156, 166). Frustules with six cingular bands, each band with a longitudinal row of slit-like areolae (Figs 158, 159). Valve mantle with scattered small areolae of irregular shape (Fig. 159).

Remarks. Observed specimens are widely variable in valve outline from clavate to linear lanceolate. Some specimens with three isolate depressions located on one side of the central area, but only one represents a stigma (Fig. 161). The external striae are formed of areolae sunk into rounded depressions (Fig. 163) which are different from non-depressed areolae in the type material (Reichardt 2001) or those illustrated by Levkov et al. (2016). This species, however, is known to have several morphotypes (Levkov et al. 2016).

Occurrence and distribution. Frequent. Previously recorded from southern Iraq (Al-Handal & Al-Shaheen, 2019).

Gomphonema procerum E.Reichardt & Lange-Bertalot (Figs 70–73, 167–175).

Reichardt & Lange-Bertalot (1991), p. 526, pl. 4: figs 1–12.

Morphology. Valves slightly heteropolar, linear-lanceolate to slightly isopolar, with narrowly rounded, unprotracted apices. Valves 36–58 µm long, 6.0–6.5 µm wide. Axial area narrow, linear lanceolate. Central area almost rectangular, bordered with a single short stria on both sides. Single isolated pore located distantly from central stria, close to proximal raphe endings. Raphe slightly lateral, proximal endings straight. Striae parallel at mid-valve, weakly radiate towards poles, 11–13 in 10 µm at mid-valve, 13–15 near poles. In the SEM, externally, raphe proximal endings straight, expanded (Figs 168, 169). Distal raphe endings slightly deflected, extending onto valve mantle (Figs 170, 172). Raphe end at foot pole bisects a well-developed apical pore field (Fig. 172). External opening of isolated pore rounded, surrounded by silica ring (Fig. 169). Areolae C-shaped, very narrow, covered by thin silica flaps (Figs 169, 171). Internally, proximal raphe endings strongly hooked, distal endings terminate in helictoglossae (Fig. 173). Isolated pore opening small, round to slightly elongated. Areolae with internal elliptical openings, arranged in deep narrow foraminal rows, separated by well-developed vimines (Figs 174, 175). Pseudosepta present on both poles (Figs 174, 175).

Occurrence. Rare. *G. procerum* was not previously reported from Iraq.

Gomphonema pumilum (Grunow) E.Reichardt & Lange-Bertalot (Figs 74–77, 176–181)

Reichardt & Lange-Bertalot (1991), p. 528, pl. 6: 4–11, Levkov et al. (2016), p. 110, pl. 151, figs 26–52.

Morphology. Valves linear-lanceolate to narrowly clavate with broadly rounded head poles and narrowly rounded to weakly protracted base pole. Valve 13–15 µm long, 3.2–4.0 µm wide. Axial area linear-lanceolate, opens to laterally transversed central area formed by single short stria from both sides. Raphe filiform, central to weakly lateral. Proximal raphe endings tear-drop-shaped, slightly elongated. Striae slightly radiate, 8–10 in 10 µm at mid-valve, 10–12 near the poles. In the SEM, externally, distal raphe endings weakly curved near the poles, becoming straight at mantle (Figs 177, 178). Raphe end at foot pole bisects apical pore field formed of large and rounded porelli (Fig. 178). Striae C-shaped, covered with silica flaps (Fig. 177). Internally, proximal raphe endings strongly hooked (Fig. 180). Distal raphe endings terminate before apices in helictoglossae (Fig. 179). Isolated pore opening located distantly from the short striae, with rounded to slightly elongated opening (Fig. 180). Striae bordering the central nodule slightly curved towards proximal raphe endings (Fig. 180). Areola openings rounded, sunk in foraminal elongated rows separated by strongly silicified vimines (Figs 180, 181).

Occurrence and distribution. Rare. Not recorded previously from Iraq.

Discussion

The material from Haqlan hot springs is rich in *Gomphonema* spp. and other diatoms despite its high sulphate concentration which reached 2040 mg/l. *Gomphonema brockiae*, *G. commutatum*, *G. contraturris* and *G. latcollum* were found in every sample examined. These were associated with other common taxa including *Crenotia thermalis* (Rabenhorst) Wojtal, *Crenotia angustior* (Grunow) Wojtal, *Ulnaria ulna* (Nitzsch) Compère, *Cocconeis placentula* Ehrenberg, *Cocconeis euglypta* Ehrenberg, *Cocconeis pediculus* Ehrenberg, *Fragilaria* spp., *Tabularia* spp., *Navicula* spp. and *Nitzschia* spp. Of the 11 *Gomphonema* species reported here, 8 were not previously reported from Iraq. All *Gomphonema* species reported here were only found epiphytic on the aquatic plant *Najas minor*, but this number may well increase if other substrates such as other macrophytes and sediments are examined.

The present work includes the description of two new species, *Gomphonema brockiae* sp. nov. and *G. hadithaensis* sp. nov. A comparison of the morphological features between these two species and the related taxa of the genus is given in Tables 1 and 2. The most similar species to *G. brockiae* is *G. incognitum* E.Reichardt, Jüttner & E.J.Cox (in Jüttner et al. 2004). The latter species has a comparable valve shape and size (broadly clavate, 17–39 µm long, 4.0–6.5 µm wide), but differences can be noticed in the stria density (9–11 in 10 µm vs. 14–16 in 10 µm in

G. incognitum). Additionally, *G. incognitum* is a typically freshwater species occurring in the streams and waterfalls, while *G. brockiae* is a thermophilic and halophilic species. *Gomphonema nepalense* Reichardt, Jüttner & E.J.Cox (in Jüttner *et al.* 2004) has larger valves (18–55 μm long and 6.0–8.0 μm wide), narrower axial areal, more elongated areolae (almost slit-like) and pores on the girdle bands interrupted in the mid-valve. *Gomphonema chinense* Liu & Kociolek (in Liu *et al.* 2013) has comparable valve size as *G. brockiae* (24.4–31.8 μm long, 4.6–5.1 μm wide), but difference can be noticed in the valve shape (linear-lanceolate with slightly protracted head pole in *G. chinense*). *Gomphonema siamense* has longer valves than *G. brockiae* (25.3–52.0 μm) and narrowly rounded to sub-cuneate head pole. Although it has a broad axial area, *Gomphonema entolejum* Østrup can be easily differentiated from *G. brockiae* by its much larger valves (37.6–78.3 μm long, 6.5–9.4 wide) and different shape of both poles.

Gomphonema hadithaensis is similar to *G. naviculoides* W. Smith (Reichardt 2015). Lectotypification of *G. naviculoides* was performed by Van de Vijver *et al.* (2020) and the species is characterized by almost naviculoid valves 28–65 μm long and 7.5–10.0 μm wide with 11–12 striae in 10 μm . Differences between *G. hadithaensis* and *G. naviculoides* can be noticed in the valve size (length 85–102 μm , width 13.0–15.0 μm vs. length 28–65 μm and width 7.5–10.0 μm , respectively). Reichardt (2015) described several new species from this complex, such as *G. graciledictum* E.Reichardt, *G. stagnorum* E.Reichardt, *G. disgracile* E.Reichardt, *G. campodunense* E.Reichardt, but all of them have much smaller valves than *G. hadithaensis*. *Gomphonema guaraniarum* Metzeltin & Lange-Bertalot (2007) has smaller valves (length 50–90 μm width 10.3–12.0 μm) and, thus, can be easily differentiated from *G. hadithaensis*. *Gomphonema vibrioides* E.Reichardt & Lange-Bertalot (1991) has similar valve shape to *G. hadithaensis*, but both species can be easily differentiated by the valve size (length 47.5–105.0 μm , width 6.7–10.4 μm). *Gomphonema archaeovibrio* Lange-Bertalot & E.Reichardt (in Reichardt 1995) has comparable valve length (75–120 μm) and shape (narrowly lanceolate) as *G. hadithaensis*, but differences can be noticed in the valve width (10.5–13.0 μm in *G. archaeovibrio*).

There is a tendency to consider the newly described freshwater *Gomphonema* species, particularly in the southern hemisphere, as endemic to the locations where they were found (Kociolek & Stoermer 2001, Vanormelingen *et al.* 2008, Karthick *et al.* 2011). Such hypothesis should be carefully applied to freshwater diatoms as some of these species might appear to be conspecific with certain old taxa from the northern hemisphere or be found later in a different geographic location. An example of such a case is presented in Van de Vijver *et al.* (2008) where a freshwater species considered as an Antarctic endemic was found later in Northern Europe. It is well known that there is a

Table 1. Comparison of the morphological features of *Gomphonema brockiae* sp. nov. to some similar species of the genus.

Features	Species					
	<i>G. brockiae</i>	<i>G. incognitum</i>	<i>G. nepalense</i>	<i>G. chinense</i>	<i>G. siamense</i>	<i>G. entolejum</i>
Valve length (μm)	19–30	17–39	18–55	24.4–31.8	25.3–52	37.6–78.3
Valve width (μm)	5.5–6.5	4–6.5	6–8.7	4.6–5.1	5.3–6.7	6.5–9.4
Valve outline (μm)	Clavate-lanceolate	Broadly elliptic, lanceolate apices	Clavate, lanceolate to elliptic-lanceolate, cymbelloid apices	Clavate, elliptic-lanceolate, rostrate apices	Linear-lanceolate, rounded to broadly apices	Linear-lanceolate, rounded apices
Axial area	Broadly lanceolate	Broadly lanceolate	Lanceolate	Broadly lanceolate	Broadly lanceolate	Broadly lanceolate
Central area	Widely rounded	Rhombic lanceolate	Rhombic	Absent	Indistinct	Absent
Raphe	lateral, undulate	Slightly lateral, undulate	Lateral, undulate	Lateral	Distinctly lateral	Lateral, slightly undulate branches
Stria density/10 μm	9–12	14–16	12–13.5	10–13	10–13	13–14
Areolae	C-shaped to slightly elongated	Mostly Sickle-shaped, some are rounded	Sickle-shaped adjacent to axial area, otherwise elongated	C-shaped	Slit-like	Slit-like
Reference	Present study	Jüttner <i>et al.</i> (2004)	Jüttner <i>et al.</i> (2004)	Liu <i>et al.</i> (2013)	Reichardt (2005)	Reichardt (2005)

Table 2. Comparison of the morphological features of *Gomphonema hadithaensis* sp. nov. to some similar species of the genus.

Features	Species					
	<i>G. hadithaensis</i>	<i>G. naviculoides</i>	<i>G. gracilidictum</i>	<i>G. stagnorum</i>	<i>G. disgracile</i>	<i>G. archaeovibrio</i>
Valve length (µm)	85–102	26–69	23–62	35–65	17–46	75–120
Valve width (µm)	13–15	7.5–10	5.5–8	7.5–8.8	5.8–7.8	10.5–13
Valve outline (µm)	Isopolar, rhombic-lanceolate, acutely rounded apices	Rhombic-lanceolate to lanceolate, acutely rounded	Rhombic-lanceolate to isopolar, rounded apices	Naviculaid, lanceolate to rhombic lanceolate, rounded apices	Rhombic-lanceolate, acutely rounded apices	Narrowly lanceolate, acute apices
Axial area	Linear, slightly wide	Linear, wide	Linear, narrow	Narrow	Narrow	Linear, narrow
Central area	small, irregular, laterally dilated	Small, indistinct	Transversely elongated	Small, lateral	Small, lateral	Absent
Raphe	Slightly undulate	Distinctly lateral	Weakly lateral	Lateral, slightly curved	Straight, filiform	Slightly lateral
Stria density/10 µm	7–9 at mid-valve, 13–15 towards apices	11–16	13–18	11–13	10–14	9–12
Areolae	Slit-like	Reniform to C-shaped	C-shaped	C-shaped	C-shaped	C-shaped
Reference	Present study	Lekov et al. (2016)	Lekov et al. (2016)	Reichardt (2015)	Reichardt (2015)	Metzeltin & Lange-Bertalot (1998)

great deal of confusion in diatom taxonomy because of narrow species concepts as well as minor variations in morphological features (Mann 1999). Phenotypic variations between populations of the same species in different geographical regions may lead to the description of new taxa (Cox 1995). In such circumstances, the diatom ubiquity hypothesis prevails which reduces the possibility of endemism.

Acknowledgements

The authors are grateful to the CMAL laboratory staff for their help with SEM. Our gratitude to the Department of Biological and Environmental Sciences, University of Gothenburg, Sweden, for providing laboratory equipment and light microscopy.

Disclosure statement

No potential conflict of interest was reported by the author(s).

Funding

This work was partially supported by the Swedish Research Council [grant number 2018-04289].

ORCID

Adil Y. Al-Handal  <https://orcid.org/0000-0003-4703-7823>

Zlatko Levkov  <https://orcid.org/0000-0002-1184-2356>

Angela Wulff  <https://orcid.org/0000-0003-0015-7019>

References

- ABARCA N., JAHN R., ZIMMERMANN J. & ENKE N. 2014. Does the cosmopolitan diatom *Gomphonema parvulum* (Kützing) Kützing have a biogeography? *PLoS One* 9: e86885.
- ABARCA N., ZIMMERMANN J., KUSBER W.-H., MORA D., VAN A.T., SKIBBE O. & JAHN R. 2020. Defining the core group of the genus *Gomphonema* Ehrenberg with molecular and morphological methods. *Botany Letters* 167(1): 114–159.
- AL-HANDAL A.Y. & AL-SHAHEEN M. 2019. Diatoms in the wetlands of Southern Iraq. In: *Bibliotheca Diatomologica*, Vol. 67, pp. 1–252.
- APHA. 2017. *Standard methods for the examination of water and wastewater*. 23rd ed. American Public Health Association, Washington, DC, USA.
- CHUDAEV D.A., KOCIOLEK J.P. & GOLOLOBOVA M.A. 2014. *Gomphonema megalobrebissonii* sp. nov.: a new large-celled taxon in species complex around *G. acuminatum* from the sediments of Lake Glubokoe (European Russia). *Nova Hedwigia* 143: 255–269.
- COX E.J. 1995. Morphological variation in widely distributed diatom taxa: taxonomic and ecological implications. In: *Proceedings of the 13th International Diatom Symposium* (Ed. by M. DONATO & M. MONTRESOR), pp. 335–345. Biopress, Bristol.
- GUIRY M.D. & GUIRY G.M. 2024. *Algaebase. World-wide electronic publication*. National University of Ireland, Galway.

- HINTON G.C.F. & MAULOOD B.K. 1979a. Freshwater diatoms from Sulaimaniyah, Iraq. *Nova Hedwigia* 31: 449–466.
- HINTON G.C.F. & MAULOOD B.K. 1979b. Some observations on the diatom flora of Serchinar spring, Sulaimaniyah, Iraq. *British Phycological Journal* 14: 175–183.
- HIRANO M. 1973. Freshwater algae from Mesopotamia. *Contribution Biology Laboratory Kyoto University* 24: 106–119.
- JAHN R, ABARCA N., GEMEINHOLZER B., MORA D., SKIBBE O., KULIKOVSKIY M., GUSEV E., KUSBER W.-H. & ZIMMERMANN J. 2017. *Planothidium lanceolatum* and *Planothidium frequentissimum* reinvestigated with molecular methods and morphology: four new species and the taxonomic importance of the sinus and cavum. *Diatom Research* 32(1): 75–107.
- JÜTTNER I., REICHARDT E. & COX E.J. 2004. Taxonomy and ecology of some new *Gomphonema* species common in Himalayan streams. *Diatom Research* 19(2): 235–264.
- JÜTTNER I., ECTOR L., REICHARDT E., VAN DE VIJVER B., JARLMAN A., KROKOWSKI J. & COX E.J. 2013. *Gomphonema varioeruduncum* sp. nov., a new species from northern and western Europe and a re-examination of *Gomphonema exilissimum*. *Diatom Research* 28(3): 303–316.
- KARTHICK B., KOCIOLEK J.P., MAHESH M.K. & RAMACHANDRA T.V. 2011. The diatom genus *Gomphonema* Ehrenberg in India: checklist and description of three new species. *Nova Hedwigia* 93(1-2): 211–236.
- KARTHICK B., YOGESHWARAN M. & KOCIOLEK J.P. 2023. A new freshwater gomphonemoid diatom genus from India, with the description of a new species from the Eastern Ghats. *Phycologia* 62(5): 499–511.
- KOCIOLEK J.P. & STOERMER E.F. 2001. Taxonomy and ecology: a marriage of necessity. *Diatom Research* 16: 433–442.
- KOCIOLEK J.P., YOU Q.-M., WANG Q.-X. & LIU Q. 2015. Consideration of some interesting freshwater gomphonemoid diatoms from North America and China, and the description of *Gomphosinica*, gen. nov. *Nova Hedwigia* 144: 175–198.
- KOCIOLEK J.P., BALASUBRAMANIAN K., BLANCO S., COSTE M., ECTOR L., LIU Y., KULIKOVSKIY M., LUNDHOLM N., LUDWIG T., POTAPOVA M., RIMET F., SABBE K., SALA S., SAR E., TAYLOR J., VAN DE VIJVER B., WETZEL C.E., WILLIAMS D.M., WITKOWSKI A. & WITKOWSKI J., 2019. DiatomBase, <http://www.diatombase.org>.
- KOLBE R.W. & KRIEGER W. 1942. Süsswasserlagen aus Mesopotamien und Kurdistan. *Berichte der Deutschen Botanischen Gesellschaft* 60: 336–355.
- KRAMMER K. & LANGE-BERTALOT H. 1986. Bacillariophyceae 1, Naviculaceae. In: *Süsswasserflora von Mitteleuropa* (Ed. by H. Ettl, J. Gerloff, H. Heynig, & D. Mollenhauer), Vol. 2/1. Gustav Fischer Verlag, Heidelberg, pp. 1–876.
- KRAMMER K. & LANGE-BERTALOT H. 1991. Bacillariophyceae: Achnanthaceae. Kritische Ergänzungen zur *Navicula* (Lineolatae) und *Gomphonema*. In: *Süsswasserflora von Mitteleuropa* (Ed. by H. Ettl, J. Gerloff, H. Heynig, & D. Mollenhauer), Vol. 2/4. Gustav Fischer, Stuttgart, pp. 1–437.
- KULIKOVSKIY M.S., KOCIOLEK J.P., SOLAK C.N. & KUZNETSOVA I. 2015. The diatom genus *Gomphonema* Ehrenberg in Lake Baikal. II. Revision of taxa from *Gomphonema acuminatum* and *Gomphonema truncatum-capitatum* complexes. *Phytotaxa* 233(3): 251–272.
- LANGE-BERTALOT H. 1993. 85 neue Taxa und über 100 weitere neu definierte Taxa ergänzend zur Süßwasserflora von Mitteleuropa, Vol. 2/1-4. 85 New Taxa and much more than 100 taxonomic clarifications supplementary to Süßwasserflora von Mitteleuropa. *Bibliotheca Diatomologica* 27: 1–454.
- LANGE-BERTALOT H. & METZELTIN D. 1996. Indicators of oligotrophy. 800 taxa representative of three ecologically distinct lake types, carbonate buffered-Oligodystrophic-weakly buffered soft water with 2428 figures on 125 plates. Oligotrophie-Indikatoren. 800 Taxa repräsentativ für drei diverse Seen-Typen. *Iconographia Diatomologica* 2: 1–390.
- LEVKOV Z., MITIC-KOPANJA D. & REICHARDT E. 2016. The diatom genus *Gomphonema* from the Republic of Macedonia. In: *Diatoms of the European inland waters and comparable habitats* (Ed. by H. Lange-Bertalot), Vol. 8, pp. 1–552, Koeltz Botanical Books, Ruggell.
- LIU Y., KOCIOLEK J.P. & WANG Q. 2013. Six new species of *Gomphonema* Ehrenberg (Bacillariophyceae) species from the Great Xing'an Mountains, Northeastern China. *Cryptogamie, Algologie* 34(4): 301–324.
- MANN D.G. 1999. The species concept in diatoms. *Phycologia* 38: 437–495.
- MAULOOD B.K. & HINTON G.C.F. 1979. Tychoplanktonic diatoms from a stenothermal spring in Iraqi Kurdistan. *British Phycological Journal* 14: 175–183.
- MAULOOD B.K., FIKRAT M.H., AL-LAMI A.A., JANAN J.T. & ABBAS M.I. 2013. *Check list of algal flora in Iraq*. Ministry of Environment, Baghdad. 94 pp.
- MEDEROS, G., AMARAL, M.W.W., PAULA, C.F., LUDWIG, T.V. & BUENO, N.C. 2018. *Gomphonema* Ehrenberg (Bacillariophyceae, Gomphonemataceae) of the São Francisco Falso River, Paraná, Brazil. *Biota Neotropica* 18(3): e20170495.
- MEDLIN L.K. & ROUND F.E. 1986. Taxonomic studies of marine gomphonemoid diatoms. *Diatom Research* 1: 205–225.
- METZELTIN D. & LANGE-BERTALOT H. 1998. Tropical diatoms of South America I: about 700 predominantly rarely known or new taxa representative of the neotropical flora. *Iconographia Diatomologica* 5: 1–695.
- METZELTIN D. & LANGE-BERTALOT H. 2007. Tropical diatoms of South America II. Special remarks on biogeography disjunction. *Iconographia Diatomologica* 18: 1–877.
- REICHARDT E. 1995. Die Diatomeen (Bacillariophyceae) in Ehrenbergs Material von Cayenne, Guyane Gallica (1843). *Iconographia Diatomologica* 1: 1–99.
- REICHARDT E. 1999. Zur Revision der Gattung *Gomphonema*. Die Arten um *G. affine/insigne*, *G. angustatum/micropus*, *G. acuminatum* sowie gomphonemoide Diatomeen aus dem Oberoligozän in Böhmen. *Iconographia Diatomologica* 8: 1–203.
- REICHARDT E. 2001. Revision der Arten um *Gomphonema truncatum* und *G. capitatum*. In: *Lange-Bertalot-Festschrift, Studies on diatoms* (Ed. by R. Jahn, J.P. Kociolek, A. Witkowski & P. Compère), pp. 187–224. A.R.G. Gantner Verlag K.G., Ruggell.

- REICHARDT E. 2008. *Gomphonema intermedium* Hustedt sowie drei neue, ähnliche Arten. *Diatom. Research* 23(1): 105–115.
- REICHARDT E. 2015. Taxonomy and distribution of *Gomphonema subtile* Ehrenberg (Bacillariophyceae) and six related taxa. *Fottea* 15(1): 27–38.
- REICHARDT E. 2018. *Die Diatomeen im Gebiet der Stadt Treuchtlingen*. Vol. 1 and 2. Bayerische Botanische Gesellschaft, München. 1184 pp.
- REICHARDT E. & LANGE-BERTALOT H. 1991. Taxonomische Revision des Artenkomplexes um *Gomphonema angustum*, *G. dichotomum*, *G. intricatum*, *G. vibrio* und ähnliche Taxa (Bacillariophyceae). *Nova Hedwigia* 53: 519–544.
- ROSS R., COX E.J., KARAYEVA N.I., MANN D.G., PADDOCK T.B.B., SIMONSEN R. & SIMS P.A. 1979. An amended terminology for the siliceous components of the diatom cell. *Nova Hedwigia* 64: 513–533.
- ROUND F.E., CRAWFORD R.M. & MANN D.G. 1990. *The Diatoms. Biology and morphology of the genera*. Cambridge University Press, Cambridge. 747 pp.
- THOMAS E.W., KOCIOLEK J.P., LOWE R.L. & JOHANSEN J.R. 2009. Taxonomy, ultrastructure and distribution of gomphonemoid diatoms (Bacillariophyceae) from Great Smoky Mountains National Park (U.S.A.). *Nova Hedwigia* 135: 201–237.
- VAN DE VIJVER B., KELLY M., BLANCO S., JARLMAN A. & ECTOR L. 2008. The unmasking of a sub-Antarctic endemic: *Psammothidium abundans* (Manguin) Bukhtiyarova et Round in European rivers. *Diatom Research* 23: 233–242.
- VAN DE VIJVER B., ECTOR L., WILLIAMS D.M. & REICHARDT E. 2020. Observations on and typification of *Gomphonema naviculoides* W.Smith (Gomphonemataceae, Bacillariophyta). *Notulae Algarum* 159: 1–7.
- VANORMELINGEN P., VERLEYEN E. & VYVERMAN W. 2008. The diversity and distribution of diatoms: from cosmopolitanism to narrow endemism. *Biodiversity and Conservation* 17: 393–405.
- ZYDAN T.A., AL-KUBAISI R.Q. & ALI F.F. 2007. The impact of underground water and sulphide water on the properties of Euphrates from Syrian borders to Heet in Anbar governorate (in Arabic). *Journal of Anbar University for Pure Sciences* 1: 1–9.